



REPUBLIC OF TÜRKİYE
ALTINBAŞ UNIVERSITY
Institute of Graduate Studies
Mechanical Engineering

**INVESTIGATION OF A GAS-TURBINE CYCLE
ENVIRONMENTAL EMISSION AND
THERMAL EFFICIENCY BY MASS AND HEAT
RECIRCULATIONS STRATEGIES**

Abathar Yaseen Khudhair AL-AMERI

Master's Thesis

Supervisor

Asst. Prof. Dr. Yaser ALAIWI

İstanbul, 2023

**INVESTIGATION OF A GAS-TURBINE CYCLE
ENVIRONMENTAL EMISSION AND THERMAL EFFICIENCY BY
MASS AND HEAT RECIRCULATIONS STRATEGIES**

Abathar Yaseen Khudhair AL-AMERI

Mechanical Engineering

Master's Thesis

ALTINBAŞ UNIVERSITY

2023

The thesis titled INVESTIGATION OF A GAS-TURBINE CYCLE ENVIRONMENTAL EMISSION AND THERMAL EFFICIENCY BY MASS AND HEAT RECIRCULATIONS STRATEGIES prepared by ABATHAR YASEEN KHUDHAIR AL-AMERI and submitted on 00/00/2023 has been **accepted unanimously** for the degree of Master of Science in Mechanical Engineering.

Asst. Prof. Dr. Yaser ALAIWI

Supervisor

Thesis Defense Committee Members:

| | | |
|--------------------------------|----------------------------------|-------|
| Asst. Prof. Dr. Yaser ALAIWI | Department of ..., University | _____ |
| Academic Title First LAST NAME | Department of ..., University | _____ |
| Academic Title First LAST NAME | Department of ..., University | _____ |

I hereby declare that this thesis meets all format and submission requirements for a Master's thesis.

Submission date of the thesis/dissertation to Institute of Graduate Studies: ____/____/____

I hereby declare that all information/data presented in this graduation project has been obtained in full accordance with academic rules and ethical conduct. I also declare all unoriginal materials and conclusions have been cited in the text and all references mentioned in the Reference List have been cited in the text, and vice versa as required by the abovementioned rules and conduct.

Abathar Yaseen Khudhair AL-AMERI

Signature



DEDICATION

I extend my heartfelt appreciation and gratitude to my supervisor, Assistant Professor Dr. Yaser ALAIWI. I dedicate this study to him as a token of my appreciation for his unwavering commitment to shaping the appropriate scientific methodology through insightful discussions and the exchange of ideas, particularly within the scope of my project. His meticulous guidance and continuous support throughout the course of this research project have been invaluable. I am also deeply grateful to all those who have been by my side on this journey. Furthermore, I would like to express my sincere thanks to my esteemed professors and the department's head for the pivotal roles they play in overseeing important responsibilities.

ABSTRACT

INVESTIGATION OF A GAS-TURBINE CYCLE ENVIRONMENTAL EMISSION AND THERMAL EFFICIENCY BY MASS AND HEAT RECIRCULATIONS STRATEGIE

AL-AMERI, Abathar Yaseen Khudhair

M.Sc., Mechanical Engineering, Altınbas University

Supervisor: Asst. Prof. Dr. Yaser ALAIWI

Date: December / 2023

Pages: 80

This The gas-turbine cycle is a power generation method that converts thermal energy into mechanical energy using a gas turbine. It involves a compressor, combustion chamber, turbine, and exhaust system, generating high-pressure, high-temperature gases. Gas-turbine cycles are utilized in power generation, aircraft propulsion, oil and gas production, and peak shaving, particularly for applications requiring rapid power ramp-up and ramp-down. Heat recirculation involves reusing exhaust gas waste heat to boost thermal efficiency by reducing heat losses, using various types of heat exchangers like counterflow, crossflow, and recuperators. Mass recirculation increases fluid flow rate, improves cycle performance, and reduces emissions by lowering combustion temperature, thereby reducing the formation of pollutants like NOx. The gas turbine is a highly adaptable turbomachinery that finds application in various vital sectors such as power generation, process plants, oil and gas, aviation, and domestic sectors. Its primary functions include compressing air and initiating fuel combustion. Gas turbines are commonly used for electricity production due to their small footprint, quick start-up, and integration with other units. The study used ANSYS and SolidWorks software to simulate a shell and tube heat exchanger. With 2090107 mesh and tetrahedral in ANSYS property. It allows detailed 3D modeling, simulation, and technical documentation generation, making it widely used in industries like aerospace and defense. When two different kinds of heat exchangers, one that operates on three tubes and the other on five tubes, were employed, and where the intermediate barriers were altered in numerous

scenarios, including once when the intermediate barriers were six, eight, and ten times. The parameters of the heat exchanger input depend on the inputs of the EES program, which includes the temperature difference across the compressor, which was taken as 745, 916, and 1055 degrees Celsius, as well as the pressure value, which represents 120 kPa and 100 kPa. Results shows that the increasing in baffles number, temperature degree and pipes leads to increase in the system performance while the increasing in pressure causing increasing in the fluid velocity but decreasing in thermal behaviour of exchanger. The system overall energy is 62.57 kW which obtained highest temperature of 471.3 oC, while the energy of the system is 60.42 at the same temperature.

Keywords: Gas Turbine, Thermal Efficiency, Mass, Emission, Exergy.

TABLE OF CONTENTS

| | <u>Pages</u> |
|---|--------------|
| ABSTRACT | vi |
| LIST OF TABLES..... | xi |
| LIST OF FIGURES..... | xii |
| ABBREVIATIONS..... | xiv |
| LIST OF SYMBOLS..... | xv |
| 1. INTRODUCTION | 1 |
| 1.1 GAS TURBINE MODEL | 4 |
| 1.2 GAS TURBINE FUELS | 4 |
| 1.3 ENVIRONMENTAL PERFORMANCE..... | 5 |
| 1.4 THE AIMS OF THE STUDY | 6 |
| 2. LITERATURE REVIEW | 7 |
| 2.1 INTRODUCTION..... | 7 |
| 2.2 GAS-TURBINE CYCLE | 7 |
| 2.3 ENVIRONMENTAL EMISSION | 12 |
| 2.4 THERMAL EFFICIENCY | 19 |
| 2.5 MASS AND HEAT RECIRCULATION'S STRATEGIES..... | 23 |
| 2.6 OBJECTIVE | 28 |
| 3. METHODOLOGY | 29 |
| 3.1 INTRODUCTION..... | 29 |
| 3.2 ANSYS PACKAGE..... | 29 |
| 3.3 GOVERNING EQUATIONS | 29 |
| 3.3.1 Standard k- ϵ Model | 29 |
| 3.3.2 Mass Equation | 30 |
| 3.3.3 Momentum Equation..... | 31 |
| 3.3.4 Energy Equation..... | 31 |

| | | |
|-----------|--|-----------|
| 3.4 | SYSTEM GEOMETRY | 31 |
| 3.5 | MESH GENERATION | 32 |
| 3.6 | CONDITIONS OF THE BOUNDARY | 33 |
| 3.7 | PROBLEM SOLUTION | 34 |
| 3.7.1 | Solution Parameters..... | 34 |
| 3.7.2 | Convergence Criteria..... | 34 |
| 3.8 | EES..... | 35 |
| 3.9 | GENERAL MASS, ENERGY, AND EXERGY EQUATIONS | 35 |
| 3.10 | THERMODYNAMIC ANALYSIS FOR BC MODEL..... | 36 |
| 3.10.1 | Compressor Model | 36 |
| 3.10.2 | Combustion Chamber Model | 37 |
| 3.10.3 | Gas turbine Model..... | 38 |
| 3.11 | ECONOMIC ANALYSIS..... | 39 |
| 3.12 | COST PERFORMANCE | 40 |
| 3.13 | SUPPOSITIONS AND INFORMATION BOUNDARY TO THE CONSOLIDATED FRAMEWORK..... | 40 |
| 4. | RESULTS AND DISCUSSIONS..... | 42 |
| 4.1 | INTRODUCTION..... | 42 |
| 4.2 | EFFECT OF BAFFLES | 42 |
| 4.3 | EFFECT OF PIPES | 46 |
| 4.4 | EFFECT OF TEMPERATURE | 48 |
| 4.5 | EFFECT OF PRESSURE | 52 |
| 4.6 | OUTLET TEMPERATURE | 55 |
| 4.7 | OVERALL EXERGY | 56 |
| 4.8 | WORK..... | 57 |
| 4.9 | ELECTRICITY | 58 |
| 4.10 | ENERGY OVERALL..... | 59 |
| 5. | CONCLUSION AND FUTURE WORKS | 60 |

| | | |
|-------------------------|-----------------------|----|
| 5.1 | INTRODUCTION..... | 60 |
| 5.2 | RECOMMENDATIONS | 60 |
| REFERENCES | 62 | |



LIST OF TABLES

| | <u>Pages</u> |
|--|--------------|
| Table 3.1: Mesh Independency..... | 33 |
| Table 3.2: Operation Condition used for the AC [23]..... | 40 |
| Table 4.1: Study Cases. | 42 |



LIST OF FIGURES

| | <u>Pages</u> |
|---|--------------|
| Figure 1.1: Industrial Waste Heat Potential Worldwide [6]..... | 2 |
| Figure 1.2: Applicable Methods for Hydrogen Production [10]..... | 3 |
| Figure 1.3: Diagram of a Gas Turbine Powered By Hydrogen With Exhaust Gas Recirculation [11]..... | 3 |
| Figure 1.4: Gas Turbine Dynamic Models For System Stability [12]..... | 4 |
| Figure 3.1: Shell and Tube Design..... | 32 |
| Figure 3.2: Mesh Generated..... | 33 |
| Figure 3.3: Flow Chart | 41 |
| Figure 4.1: Temperature at 6 Baffles..... | 43 |
| Figure 4.2: Temperature at 8 Baffles..... | 43 |
| Figure 4.3: Temperature at 10 Baffles..... | 43 |
| Figure 4.4: Pressure at 6 Baffles..... | 44 |
| Figure 4.5: Pressure at 8 Baffles..... | 44 |
| Figure 4.6: Pressure at 10 Baffles..... | 44 |
| Figure 4.7:Velocity at 6 Baffles. | 45 |
| Figure 4.8:Velocity at 8 Baffles. | 45 |
| Figure 4.9:Velocity at 10 Baffles. | 45 |
| Figure 4.10: Temperature at 3 Pipes..... | 46 |
| Figure 4.11: Temperature at 5 Pipes..... | 47 |
| Figure 4.12: Pressure at 3 Pipes. | 47 |
| Figure 4.13: Pressure at 5 Pipes. | 47 |
| Figure 4.14: Velocity at 3 Pipes. | 48 |

| | |
|--|----|
| Figure 4.15: Velocity at 5 Pipes. | 48 |
| Figure 4.16: Temperature at 745 °C. | 49 |
| Figure 4.17: Temperature at 916 °C. | 49 |
| Figure 4.18: Temperature at 1055 °C. | 50 |
| Figure 4.19: Pressure at 745 °C. | 50 |
| Figure 4.20: Pressure at 916 °C. | 50 |
| Figure 4.21: Pressure at 1055 °C. | 51 |
| Figure 4.22: Velocity at 745 °C. | 51 |
| Figure 4.23: Velocity at 916 °C. | 51 |
| Figure 4.24: Velocity at 1055 °C. | 52 |
| Figure 4.25: Temperature at 1055 °C + 100 ps. | 53 |
| Figure 4.26: Temperature at 1055 °C + 120 ps. | 53 |
| Figure 4.27: Pressure at 916 °C + 100 ps. | 54 |
| Figure 4.28: Pressure at 916 °C + 120 ps. | 54 |
| Figure 4.29: Velocity at 1055 °C + 100 ps. | 54 |
| Figure 4.30: Velocity at 1055 °C + 120 ps. | 55 |
| Figure 4.31: Outlet Temperature Diagram. | 56 |
| Figure 4.32: Exergy Diagram. | 57 |
| Figure 4.33: Work Net Diagram. | 57 |
| Figure 4.34: Electricity Diagram. | 58 |
| Figure 4.35: Overall Energy Diagram. | 59 |

ABBREVIATIONS

| | | |
|------|---|--|
| GT | : | Gas Turbine |
| DLE | : | Dry Low Emission |
| IGCC | : | Integrated Gasification Combined Cycle |
| PFBC | : | Pressurized Fluidized Bed Combustion |
| ERC | : | Ejector Refrigeration Cycle |
| NOx | : | Nitrogen Oxides |
| EGR | : | Exhaust Gas Recirculation |
| RSM | : | Response Surface Methodology |
| AT | : | Ambient Temperature |
| TIT | : | Turbine Inlet Temperature |
| TE | : | Thermal Efficiency |
| GTC | : | Gas Turbine Cycle |
| GTIT | : | Gas Turbine Inlet Temperature |
| DAC | : | Double Annular Combustors |
| ITES | : | Ice Thermal Energy Storage |

LIST OF SYMBOLS

| | |
|--------------------|---|
| m_p | : Mass Commitment to the Mass Hotspot for Phase p |
| $m_{pq'}$ | : Mass Flow Rate from Phase P to Another Phase Denoted by Q' |
| \vec{u}_p | : Velocity Vector of Phase p |
| m_{piq} | : Specific Mass Flow Rate Between Different Phases or Stages |
| m_q | : Mass Commitment for Phase Q |
| m_{pqq} | : Transfer Rate Within Phase Q or from Phase P to Phase Q |
| H_p | : Energy Source in a Cell for Phase P |
| $h_q^{f^i}$ | : Enthalpy of Phase Q at Some State f^i |
| $h_p^{f^k}$ | : Enthalpy of Phase p at Some State f^k |
| $h_p^{f^i}$ | : Enthalpy of Phase P at State f^i |
| \dot{m}_{in} | : Mass Flow Rate Entering a Control Volume |
| \dot{m}_{out} | : Mass Flow Rates Exiting a Control Volume |
| \dot{Q} | : Heat Transfer into the System |
| \dot{W} | : Work Transfers out of the System |
| h_{in} | : Specific Enthalpy of Inflow |
| h_{out} | : Specific Enthalpy of Outflow |
| \dot{E} | : Rate of Total Energy Transfer in a System or Control Volume |
| ψ | : Maximum Useful Work Obtainable from a Flow Process |
| s | : Specific Entropy of the Fluid at a Given State. |
| s_0 | : Reference Specific Entropy at the Standard State. |
| η_{AC} | : Efficiency of an Air Conditioning System |
| P_{AC} | : Power Associated with an Air Conditioning System |
| ε_{AC} | : Emissivity |
| CRF | : Acronym |

1. INTRODUCTION

The effectiveness of waste heat recovery in industrial thermal processes is being improved, which will increase the efficiency of fuel utilization as concerns about fuel scarcity and environmental degradation grow [1]. According to reports, the operations of burning fuel and transferring heat squander about 63% of the primary energy used globally. Notably, a significant portion of the unused energy is found to be recoverable unused thermal energy [2]. Therefore, it is necessary and essential to do research on the use of waste thermal energy. It has been accomplished to raise public awareness of the ecological and climatic harm brought on by years of extreme energy use fueled by fossil fuels. Many nations are currently developing ways to restrict fuel intake and pollutant releases, limiting the anthropogenic influence, in accordance with well-known international conventions [3]. Usable waste and renewable thermal heat are frequently derived from sources such as data centres, diverse industrial operations, fuel-driven main movers, and renewable heat energy [4]. Enhancing the thermodynamic and environmental efficiency of electric utilities has received a lot of attention lately. Because of the increasing obtainability of natural gas, particularly by means of natural gas extraction produced by the overall fracking process, gas turbine-based electrical utilities are becoming more important in comparison to coal-based power services [5]. The potential for industrial waste heat and the overall amount of energy consumed by nations globally are shown in Figure 1.1. Recovery of waste heat from manufacturing processes is more difficult than recovering waste heat from marketable or residential structures. Due to the fact that most industries are situated far from where consumers are, there are problems with thermal energy storage and transportation [6].

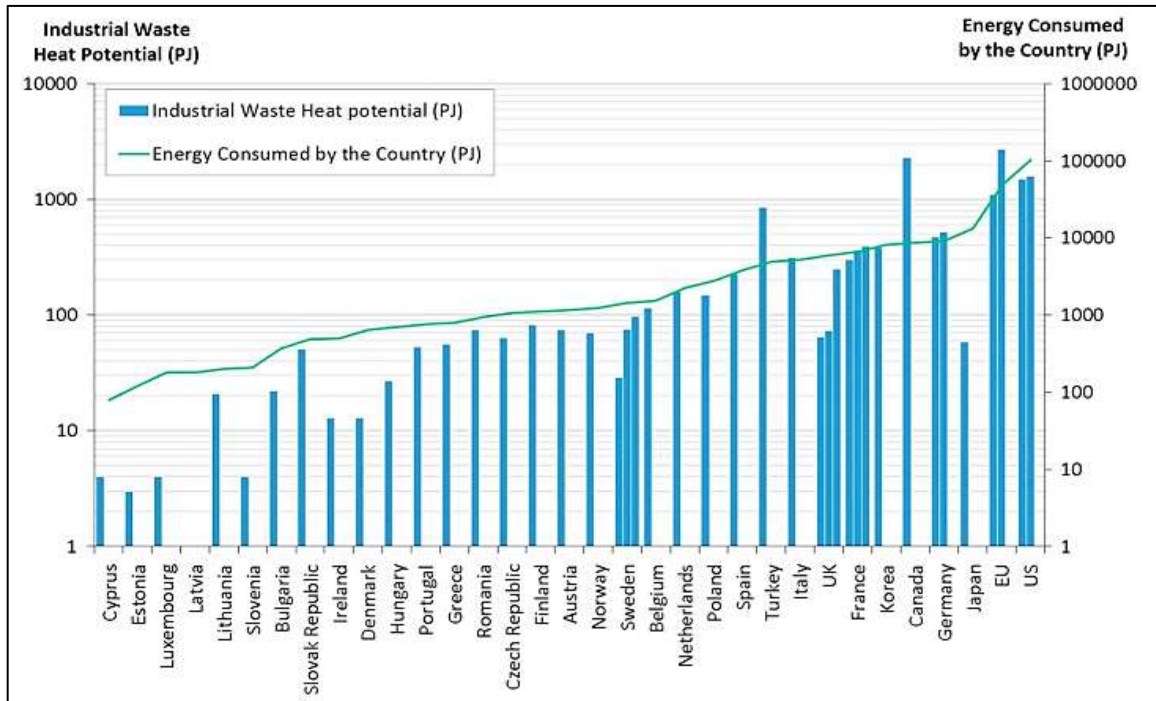


Figure 1.1: Industrial Waste Heat Potential Worldwide [6].

Gas turbines (GTs) are commonly utilized in the field of electricity generation due to their favorable characteristics. These include their ability to provide significant power output in a compact physical footprint, their quick start-up time, and their potential for integration with other energy production systems like Rankine cycles. Gas turbines are mostly utilized for the purpose of generating energy by employing Brayton cycles. The essential elements comprising the Brayton cycle encompass its compressor, combustor, and gas turbine [7]. The specific characteristics of the combustion process have an impact on the performance of gas turbine cycles. The type of fuel utilized in the combustion engine is a crucial factor that significantly impacts the efficiency of combustion and the resulting emissions in this particular process. In the past, fossil fuels such as oil and gas constituted the primary sources of fuel utilized in the combustion processes of these cycles[8]. Hydrogen can be produced using a variety of feedstocks, natural gas, including coal, and renewable energy resources like biomass. Many process technologies, including biological, photolytic, chemical, and thermo-chemical ones, can be used to create hydrogen. The techniques for producing hydrogen are shown in Figure 1.2. Fossil fuel reforming accounts for the largest portion of the present hydrogen production among these technologies [9].

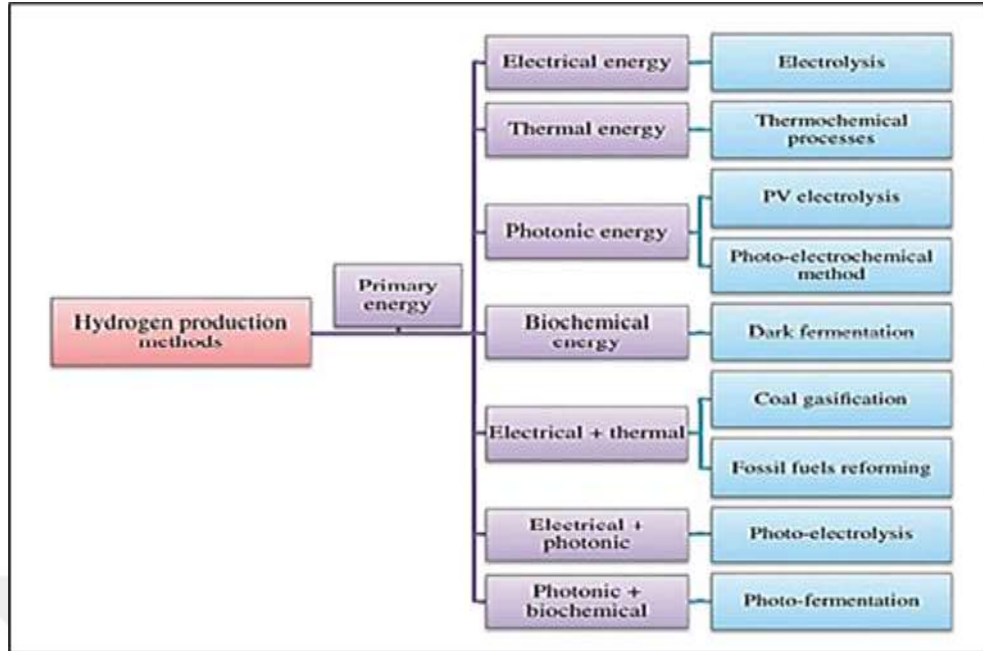


Figure 1.2: Applicable Methods for Hydrogen Production [10].

For instance, Ditaranto suggested a brand-new design called exhaust gas recirculation, which is depicted in Figure 1.3. The oxygen-depleted flow will enter the combustor in this configuration, reducing the reactivity of the H₂-rich fuel. This technique can be used to reduce NO_x generation without compromising the flame's stability. The dilution composition may have an impact on the cycles' effectiveness [11].

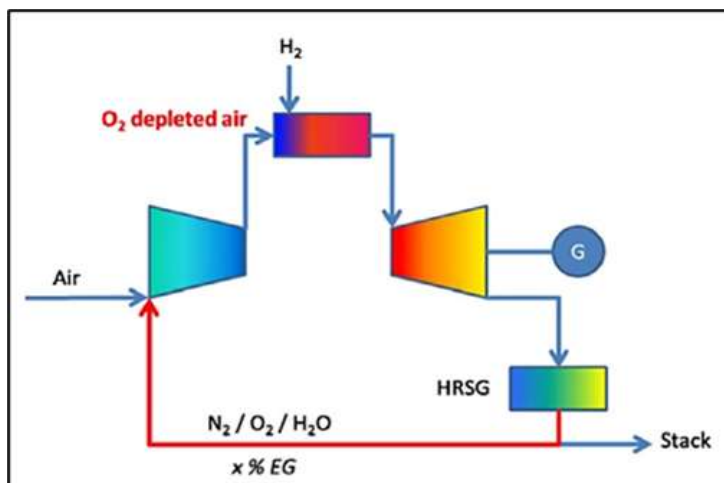


Figure 1.3: Diagram of a Gas Turbine Powered by Hydrogen with Exhaust Gas Recirculation [11].

1.1 GAS TURBINE MODEL

These difficulties with DLE gas turbines have been addressed in numerous ways during the past few years. Several research projects concentrate on the static stability of the flame, including combustion efficiency, fuel injection adaptability, turbine burners, fuel flow aerodynamics, fuel combustion, and fuel mixing. Analyzing the works reveals that the majority of them are concerned with combustor design, combustion fuels, or the combustion process. Only a few studies consider the control strategy and the system as a whole. Also, the majority of the work is exclusively done in laboratories. Also, Figure 1.4 illustrates the specific dynamic models for the analysis of gas turbine stability [12].

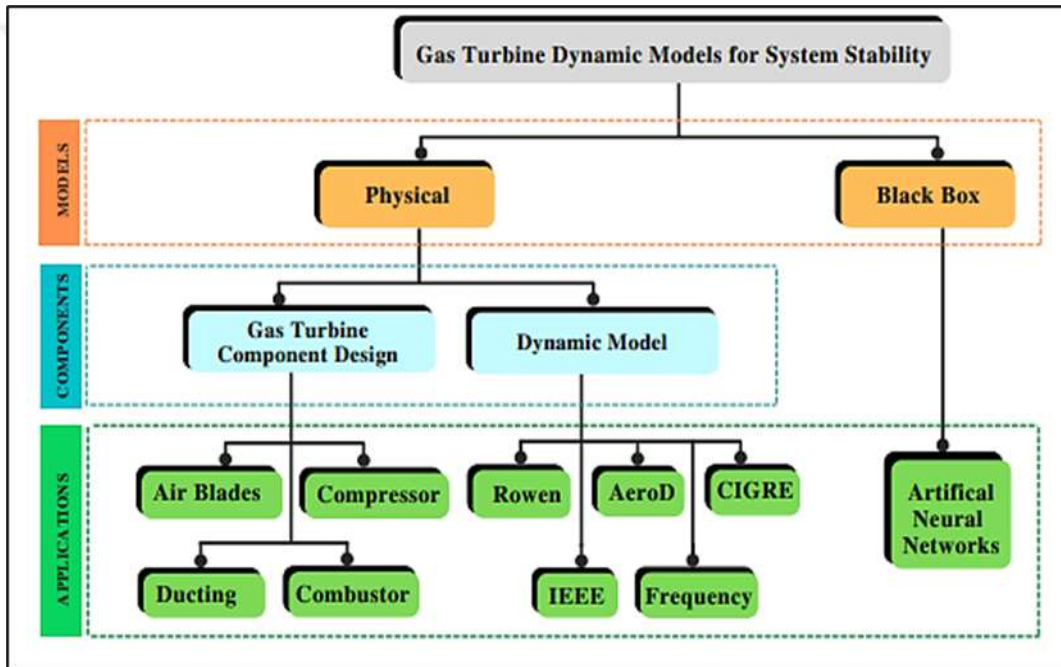


Figure 1.4: Gas Turbine Dynamic Models for System Stability [12].

1.2 GAS TURBINE FUELS

In contemporary times, industrial gas turbines predominantly combust a variety of fuels, including propane, butane, blast furnace gas, petroleum distillates, natural gas, and residual fuel oil. Presently, there are ongoing endeavours to enable gas turbines to operate utilizing solid fuels such as coal and biomass. Methanol, hydrogen, and vegetable oil have been identified as potential alternative fuel sources for gas turbines.

[13]. One possibility is the development of technologies for gasifying coal and biomass to create a clean gas that may be burned directly in a gas turbine compressor. Systems with integrated gasification combined cycle (IGCC) use this technology. Alternatives for gasification for gas turbine-based power production include bagasse, an organic waste product from the sugar manufacturing sector, a mixture of leftover cooking chemicals, and organic components from the chemical pulp cooking process [14]. Pressurized fluidized bed combustion, or PFBC, is another option for incorporating solid fuel combustion in the gas turbine system. Here, a fluidized bed combustion engine receives compressed air from a gas turbine compressor. The hot combustion yields are expanded in a turbine, and a steam turbine bottoming cycle recovers the exhaust heat [15]. The PFBC method is primarily thought to be appropriate for coal. Utilizing a superficially (or indirectly) fired gas turbine provides a third option. Combustion byproducts never come into close contact with the gas turbine in an externally fired gas turbine. Instead, the heat from the combustion products is transferred to an air-based working fluid that powers the turbine via a high-temperature heat exchanger. The need for fuel cleaning can be reduced in this way [16].

1.3 ENVIRONMENTAL PERFORMANCE

In contrast, gas turbines emit very little pollution, especially when running on natural gas. The low emissions per unit of generated usable energy are a result of their high efficiency, particularly when running in combined cycle or cogeneration mode. Many air contaminants, including NOx, CO, and organic compounds, can be considerably decreased by making variations to the combustion process [17]. Significant efforts have been made to create various emission-lessening strategies, particularly low-NOx gas turbines. Before the fuel gas is burned, sulfur-containing impurities can be removed by the gasification of solid fuels. In pressured fluidized bed combustion, sulfur emitted during combustion is captured using a sorbent like dolomite or limestone. The use of combustion systems with minimal emissions, such as atmospheric fluidized bed combustion systems, can be combined with externally fired gas turbine systems [18]. One emerging area of research pertains to the mitigation of carbon dioxide (CO2) emissions stemming from gas turbine operations. Research in this particular domain has predominantly concentrated on two methodologies: the first involves facilitating the operation of the gas turbine using a fuel source that is carbon dioxide (CO2)-neutral, such as biomass. The second technique is utilizing fossil fuels as the primary energy

source while simultaneously trapping CO₂ emissions and preventing their release into the environment [19].

1.4 THE AIMS OF THE STUDY

The following are the goals of research into heat and mass recirculation techniques for raising a gas-turbine cycle's thermal efficiency and emissions:

- i. To determine and assess the advantages and restrictions of mass and heat recirculation techniques in gas-turbine cycles.
- ii. To ascertain the ideal set-up and design specs for gas-turbine cycles' heat and mass recirculation systems.
- iii. The purpose of this study is to quantify the enhancements in thermal efficiency and reductions in emissions resulting from the implementation of mass and heat recirculation techniques in gas-turbine cycles.
- iv. To create fresh, enhanced heat and mass recirculation techniques that boost gas-turbine cycles' thermal performance and lower emissions.
- v. To offer helpful suggestions for putting heat and mass recirculation techniques into action in gas-turbine cycles to boost thermal efficiency and cut emissions.

2. LITERATURE REVIEW

2.1 INTRODUCTION

The examination of a gas turbine cycle's natural discharge and warm productivity by mass and intensity distribution techniques is a significant area of exploration in gas turbine studies. Mass and intensity distribution methodologies include recycling fumes, gases, and waste intensity back into the gas turbine cycle, which can work to increase productivity and decrease discharges. A few studies have researched the viability of mass and intensity distribution techniques on gas turbine cycles. examined the utilization of fume gas distribution and steam infusion in a gas turbine cycle. The investigation discovered that EGR could decrease NOx outflows by up to 80% while keeping up with warm productivity, and steam infusion could increment warm effectiveness by up to 6% while diminishing discharges. The utilization of an intensity exchanger in a gas turbine cycle to recycle waste heat. The investigation discovered that the utilization of an intensity exchanger could increase warm proficiency by up to 8%, decrease fuel utilization, and lessen discharges.

Generally speaking, the utilization of mass and intensity distribution systems in gas turbine cycles can possibly work on both the natural execution and the warm proficiency of gas turbines. Notwithstanding, the viability of these methodologies relies upon a few elements, for example, the particular gas turbine configuration, working circumstances, and the sort of distribution methodology utilized. More research should help make mass and intensity distribution systems more useful in gas turbine cycles and help make sure that these methods are carried out in a way that makes sense.

2.2 GAS-TURBINE CYCLE

The study conducted by Du et al. (2021) [20] investigated the GT-KCS-ERC, a novel integrated power-cooling system that incorporates the gas turbine, Kalina cycle structure, and ERC, which is limited by the availability of GT pipe gas and KCS low-obsession liquid waste energy sources. Thermodynamic and thermo-monetary calculations are performed to show the structure's possibility, and Non-managed Orchestrating Innate Estimation II is used for the multi-objective progression. The disclosures show that the overall energy capability of the system improves with the rising press point temperature differential of pot TKCS, boi,

and decreasing smelling salt content of the working course of action in KCS. In addition, the LCOE of the structure is lower than that of the autonomous system, and the structure outmanoeuvres the free structure similarly as cooling breaking point and net power when the ERC discretionary stream split extent is 0.162 for precooling GT confirmation air.

Ding et al. (2021) [21] The study examined the utilization of the gas turbine cycle as the primary framework, along with the incorporation of the Kalina cycle and the humidification-dehumidification desalination unit as the subsystems for waste intensity recovery.

The utilization of advanced Exergoeconomic evaluation and progressed exergy analysis is employed to evaluate and contrast the results obtained from a gas turbine cycle located in Inchon, South Korea, as conducted by Uysal and Keçebaş (2021) [22]. Both approaches showed that a greater percentage of the system's energy destruction cost rate was inevitable and that the cost of needless energy destruction was greater than the cost of avoidable parts. The methods used to find a gas turbine system that was affordable were impacted by this circumstance. The strategy suggested lowering the investment cost rate for gas turbines, but the total cost of energy destruction for system components was greater than the cost for the system as a whole. The results achieved with the technique were more consistent.

Zoghi et al. (2021b) [23] examined how the framework's thermodynamic effectiveness fairly declines with an expansion in direct ordinary irradiance (DNI), yet it performs better concerning the economy and the climate. The warming creation rate diminishes as the GTC blower's tension proportion rises, and the framework's presentation experiences a financial and natural viewpoint. The net power yield and multigenerational energy effectiveness arrive at their most extreme levels at pressure proportions of 14.6 and 11.2, respectively. The age pace of intensity from an intensity recuperation steam generator (HRSG) must be incredibly expanded by raising the squeeze temperature differential.

Smelling salts are a zero-carbon fuel that is exceptionally wanted for use in gas turbine innovation, Božo et al. (2021) [24] . A straightforward humidified-smelling hydrogen Brayton cycle might bring about in general plant efficiencies of around 34%; however, more headways are important to make these units serious with the present fossil-based plants. This study means to outline the execution of a muddled cycle mathematically and logically. A two-shaft, switch Brayton gas turbine plant office was outfitted with an essential gas turbine cycle, and a Rich-Extinguish Lean framework was incorporated to improve ignition and

lower outflows. The general effectiveness has filled enormously in contrast with the fundamental turbine office, with a value of 59%. The outcomes show a huge potential for the utilization of smelling salt-based mixes with steam infusion in gas turbine offices by using state-of-the art cycles that consider lower weakening in the burning area related to state-of-the-art alkali ignition frameworks and trigeneration ideas.

Ahmadi et al. (2020) [25] directed a mathematical investigation of energy and exergy for a gas turbine cycle connected with an ORC cycle. Energy and exergy examination uncovered that dimethyl carbonate and o-xylene met the most and least positive standards, individually, and that the greatest strain accessible was the best working tension. Dimethyl carbonate was found to be the best working liquid.

Koç et al. (2020) [26] evaluated the power, heat, and energy efficiency of crucial gas turbine cycles at 50 MW power yield and 450 °C turbine outlet temperature. The system was dissected for the use of pure hydrogen and combustible gas as fuel. Examination uncovered that, up to 18 bar pressure, the recuperative cycle's capability was more conspicuous than that of the fundamental gas turbine cycle. The usage of hydrogen in gas turbine cycles gives benefits over oil gas concerning execution, the environment, and CO₂ outpouring, notwithstanding the fact that it costs more per unit of power conveyed. The base fuel costs were handled as 0.345 and 0.075 \$/kWh at 20 bars for direct gas turbine cycles, respectively. The 50 MW gas turbine's CO₂ radiation for oil gas was found to go from 46.27 to 71.15 tons CO₂/h.

Mohammadi et al. (2020) [27] broke down the power age, warm, and energy efficiencies of fundamental and recuperative gas turbine cycles at consistent power yield (50 MW) and turbine outlet temperature (450 °C). For the circumstances of using both oil gas and pure hydrogen as a fuel, the capability of the recuperative cycle was seen as better compared to that of the fundamental gas turbine cycle up to 18 bar pressure. H₂ is more ideal than oil gas with respect to execution, the environment, and CO₂ transmission, while having a more critical cost for every unit of force conveyed. The irrelevant fuel costs for involving H₂ and combustible gas are still hanging out there to be 0.345 and 0.075 dollars per kWh at 20 bars for fundamental gas turbine cycles, independently. Other than zero CO₂ radiation while utilizing H₂, the CO₂ surge of the 50 MW gas turbine was found to go from 46.27 tons to CO₂/h using petrol gas.

Budiyanto et al. (2020) [28] examined the optimal state of a propulsion system utilized in the context of liquefied natural gas. The case study focused on the utilization of the standard "Combined Gas Turbine Electric and Steam LM2500 25 MW propulsion system on the HZ LNG Carrier ship" . The exergy analysis was conducted utilizing the Engineering Equation Solver, while the exergo-environmental analysis, a sort of environmental effect assessment, was carried out employing SimaPro. The findings indicated a notable enhancement in energy efficiency of 60.93%, accompanied by a thermal efficiency of 46.78%. Additionally, there was a reduction observed in the exergo environmental percentage, which decreased to 29.98%. The Approach for Order of Preference by Comparison to Ideal Solution method was employed for enhancing the multi-objective problem.

Zhang et al. (2020) [29] proposed a novel waste intensity recuperation technique in view of the Kalian and gas turbine cycles. The assessment of the framework's energy, exergy, and ecological effects is finished to measure how well it is functioning. Different streamlining processes are completed using hereditary calculations. The TEOD (Warm Proficiency Advancement Plan) mode, which increments warm productivity and exercise effectiveness by 46.11% and 47.24%, may give the best presentation. The burning chamber contributes the most to the framework's general exergy obliteration rate, with 27141 kW, while the Kalina subsystem comes in second with a worth of 6932 kW. The LTE esteem is currently 60113 kg/kW.

Mishra et al. (2020)[30] dissected the basic gas turbine cycle (SGT) and improved the information factors for the best presentation appraisal. Reaction surface strategy (RSM) is utilized to assess the best information factors. The ideal upsides of warm effectiveness, levelheaded productivity, mass of coolant, and gas turbine explicit work are individually 39.03 percent, 36.98 percent, 0.0665 kg/kg of air, and 363.59 kJ/kg. The consequences of the gas turbine cycle code reaction and the ideal worth accomplished utilizing reaction surface methodology have been seen within a blunder scope of 0.14 percent (min.) to 0.6 percent (max.). With lower surrounding temperatures (293 K), higher objective efficiencies have been accomplished, yet the most noteworthy normal efficiencies (>36.5%) might be achieved at lower turbine bay temperatures (1470 K).

Mikielewicz et al. (2019) [31] inspected the direct gas turbine cycle (SGT) using a response surface framework (RSM). Turbine confirmation temperature (TIT), blower pressure extent

(rp), including temperature (AT), and encompassing relative dampness (RH) were considered for the evaluation of the best cycle execution limits. Warm adequacy, rational efficiency, coolant mass, and gas turbine express work have ideal potential gains of 39.03 percent, 36.98 percent, 0.0665 kg/kg of air, and 363.59 kJ/kg, independently. Looking at gas turbine cycle input factors at a turbine bay temperature of 1476.76 K, blower pressure extent of 19.8788, incorporating a temperature of 288 K, and relative dampness of 53.03 percent the gas turbine cycle code response disclosures and the ideal worth from the response surface technique have been seen inside a slip-up edge of 0.14 percent (min.) to 0.6 percent (max.). The ideal value of sensible capability may be achieved at a turbine utilization temperature of 1470 K, which is lower than the encompassing temperature of 293 K.

Khan and Tlili (2019) [32] thought about three joint gas turbine cycle plans, S3, S4, and S5, as well as clever pairings of the fundamental gas turbine cycle and the regenerative gas turbine cycle. The thermodynamics customary energy and exergy investigation is utilized to assess what the different arrangements mean for the joined cycle plant's proficiency and exergy annihilation. The discoveries show that the third plan, assigned S5, is the most worthwhile for industrialists, and the main framework plan with a minimal measure of energy misfortune is perceived and recognized utilizing the insightful methodology. This exploration gives a new elective system for expanding a power plant's net result and warm proficiency while using a similar amount of fuel.

Specific evaluation of a direct internal changing solid oxide power module (DIR-SOFC) and a gas turbine (GT) system, Leal et al. (2019) [33] The particular survey integrates an energy and exergy assessment of the crossbreed cycle utilizing the methane steam-changing cooperation's Gibbs ability minimization procedure. Assessments considering amicability are used to conclude the power module's practical current thickness and the extents of the steam-to-carbon extent at the confirmation. An automatic encounter is used to overview a blend structure containing a DIR-SOFC and a GT. The hybrid cycle achieves high energy efficiency (around 62%) and exergy capability (around 58%) (around 38%). The power extent (assessed for SOFC/GT) was 1.5. Exactly when the GT transformed into the fundamental wellspring of power, the energy unit power age lessened by commonly 7%. Nevertheless, when the power module yield declines, so does the system's energy capability.

Bontempo and Manna's (2019) [34] improved gas-turbine cycles are theoretically analyzed in this study. Three cycles are specifically examined: reheat, intercooled, and intercooled. The polytropic efficiency gains of compressors and turbines are responsible for quantifying the inherent irreversibility's associated with compression and expansion operations. This study introduces novel analytical formulations for determining the optimal overall as well as intermediate ratios of pressure that optimize the network of each of the aforementioned cycles. The network (or thermal efficiency) is increased by 34.899 percent during the reheat cycle, compared to 31.477 percent during the intercooled cycle. The intercooled and reheat cycle's maximal network is twice that of the basic cycle, and its maximum thermal efficiency results in a 24.966 percent increase over the straightforward cycle.

Zhu et al. (2019) [35] examined the performance of humidified gas turbine cycles using two different air saturator designs. Indirect evaporative coolers and Maisotsenko cycles were coupled to create Type 1 air saturators, while Type 2 was a more traditional indirect evaporative cooler. The air saturator modeling took into consideration a thorough investigation of heat and mass transmission, and parametric tests showed how the performance of various designs was affected by the system intake air temperature, turbine inlet temperature, water injection rate, and part-load ratio. When compared to Type 2 air saturators at design and 50 percent part-load ratio circumstances, the use of Type 1 water saturators yielded system efficiency improvements of 9.34 percent and 23.55 percent, respectively. This reaffirmed the advantages of using the Maisotsenko cycle to improve system efficiency.

2.3 ENVIRONMENTAL EMISSION

Jehandiseh et al. (2021) [36] further developed their investigation based on a crossbreed plan of a multi-influence scattering desalination plant with steam development and a solid oxide energy part gas turbine (SOFC-GT). It is analysed to see if the plant can make freshwater by utilizing the abundance force. The thermodynamic associations dealing with the structure's many parts are presented, and the regular assessment is driven. The effects of system execution factors, for instance, fuel usage coefficients, blower pressure extents, fuel pre-further developing rates, and steam to carbon extents, are reviewed on the speeds of CO₂, CO₂, and NO_x outpouring. The results showed that when the blower pressure extent, fuel usage coefficient, and energy unit exhaust temperature were extended, the CO/NO_x

release rates and related social costs decreased, yet as the steam to carbon extent rose, so did the recovery rate, fuel cellhouse temperature, and focused gas surge rates.

Zoghi et al. (2021a) [37] expected to recuperate the waste intensity from a mix gas turbine cycle (GTC) and air lining cycle (ABC) to drive a natural Rankine cycle (ORC). Using the three subsystems increases net power creation by 8.9%, energy and exercise effectiveness by 13.39%, and the cost rate by 7.26%. The framework's examination showed that adding the subsystems to the fixing cycle brings about a diminishing in the general framework's compensation time and natural list. Furthermore, an ascent in the GTC's blower pressure proportion (CPR), direct typical irradiance (DNI), and gulf temperature (GTIT) brings about a fall in the framework's thermodynamic execution as well as an improvement in its financial and natural execution. The framework's monetary exhibition increments as an outcome of the progressions demonstrated.

Cao et al. (2021) [38] inspected and improved an exceptional triple merged power cycle constrained by cross variety biomass-sun situated energies with respect to efficiency, cost, and regular impact. The proposed system joins a shut Brayton cycle and a Rankine cycle as the fixing cycles, with a gas turbine constrained by biomass. Exergoeconomic assessment is used to review system execution, and multi-objective improvement is used to determine the best working limits. The revelations showed that solidifying sun-situated hydrogen creation with a biomass-based gas turbine in a general sense diminishes CO₂ releases, increases power delivery breaking points, and uses less biomass. The proposed triple-joined cycle achieves an exercise capability of 30.44 percent with a LCOE of 61.37 MWh and CO₂ radiation of 0.4579 kg/kWh under the best working circumstances.

Cen et al. (2021) [39] presented a functional plausibility investigation for a creative mixture of a biomass-planetary group plan that involves sunlight-based energy for the production of hydrogen. The proton trade layer electrolyze produces hydrogen utilizing the electrical energy delivered by the photovoltaic-warm boards. It is proposed that the hydrogen created be utilized as an extra fuel in the post-terminating period of a biomass-filled gas turbine plant. To examine the framework's presentation, an Exergoeconomic examination is finished, and enhancement is finished utilizing the leveled cost of force as the objective. The presentation of the proposed framework is likewise divergent from that of a conventional biomass-powered consolidated cycle without hydrogen. Under ideal

conditions, coordinating hydrogen would prompt a 22.7% decline in carbon dioxide outflows and a 24.1% expansion in the power-creating limit with regards to a proper biomass input rate. Nonetheless, the levelized power cost for the proposed framework is more noteworthy than that for the customary framework.

Shakib et al. (2021) [40] took a gander at the usage of waste power recovery in a gas turbine cycle for warm desalination machines. It encourages a thermodynamic, exergy, and Exergoeconomic model, and six decisions are suggested depending upon the relationship between the data and result streams. The Genetic Estimation (GA) is used to overhaul the disclosures, and two separate relationship procedures are used. The use of medication TVC cooling water as the RO structure feed water is the best plan out of the six, to the extent that it has the most insignificant creation costs of the two techniques. GHG assessment showed that NOx, SO3, SO2, and CO2 decreased to 165.53, 783 ppm, and 10.5 percent of the volume segment, independently.

Wang et al. (2021) [41] introduced a progressive incorporated cooling, warming, and power framework structure utilizing a gas turbine cycle, a supercritical CO2 (sCO2) cycle, an ingestion refrigeration chiller, a steam generator, a natural Rankine cycle (ORC), and extra thermoelectric generator modules. The framework's warm effectiveness was viewed as 67.88 percent, its energy proficiency as 42.62 percent, its complete expense rate as 10.60 \$/h, and its general outflows as 923.55 kt CO2. A correlation examination uncovered that the reconciliation of the sCO2 cycle and ORC performed better financially than the recommended framework structure, which had predominant thermodynamic execution.

Yazdi et al. (2020) [42] studied the cooling of the intake air of a gas turbine power plant for four Iranian towns that reflect a variety of climatic conditions. The impacts of utilizing absorption chillers, heat pumps, and inlet fogging systems were examined. The absorption chiller was found to increase gas turbine net power by 18%, energy efficiency by 5.5%, and exercise efficiency by 2.5%. The heat pump system was found to be the best cooling system for cities with hot climates, reducing NOx pollution emissions by 60% and 53%, respectively. Inlet air cooling was found to reduce the cost of generating power in those two cities by 6.5% and 6.0%, respectively. Only dry places exhibit good performance.

Görgülü et al. (2020) [25] reviewed the introduction of gas turbines on account of water implantation high up before the blower. Two specific gas turbine systems, one non-recuperative and the other recuperative, were inherent in the investigation. The amount of water implanted was extended from 0 kg/s to 46 kg/s for the use of hydrogen as a fuel, and the data pressure of the GT-Turbine was raised from 4 bar to 20 bar. The presentation of the gas turbine systems was dissected for these conditions, and the most raised net power result, warm and exergy, was not completely settled at 58,459 kW, 22.33 percent, and 23.07 percent at 20 bar and 0.057 injected water/air mass stream extent.

Javadi et al. (2020) [43] examined how the extension of water to the air before the blower influenced the display of gas turbines. The amount of water implanted was extended from 0 kg/s to 46 kg/s, and the GT-Turbine utilization pressure was raised from 4 bar to 20 bar to use hydrogen as a fuel for the normal gas turbine structures. The practicality of the gas turbine structures was dissected relating to the implanted water-air mass stream extent and the recuperative gas turbine system's most raised net power result, warm, and exergy still hanging out there to be 131,307 kW, 50.16 percent, and 52.70 percent, independently.

Khaliq et al. (2019) [44] changed the burning gas turbine plant's approaching air by utilizing a Brayton refrigeration cycle, which is itemized in this paper's finished thermodynamic display. To determine the impacts of working elements like extraction pressure proportion, removed mass rate, turbine delta temperature, surrounding relative dampness, and mass of infused water on the thermo-ecological execution of the gas turbine cycle, vivacious assessment was combined with the emanation calculation. An examination of the proposed gas turbine cycle showed a vigorous result of 33% instead of 29% for the fundamental situation. The proposed acclimation to the fundamental gas turbine shows a critical lessening in the cycle's exergy misfortune, a huge drop in the blower's neighbourhood irreversibility, and an expansion in burning irreversibility from 19 to 21 percent. Furthermore, the ascent in surrounding relative dampness from 20 to 80 percent results in a fundamental decline in NOx fixation and a scarcely distinguishable expansion in CO focus.

Tahmasebzadehbaie et al. (2017) [18] studied a gas-turbine cycle's warm proficiency and outflow, which were expanded by considering mass and intensity distributions. Three potential situations were analyzed: simply mass dissemination, alone intensity distribution, and synchronous utilization of the two types of distribution. Multi-objective advancement

was utilized to determine the most elevated conceivable improvement. The ideal intensity was still up in the air in the circumstances when there was basically heat dissemination (AHP). At last, the AHP approach was utilized to pick the best situation for improving the gas cycle. The situation that utilized PFHE without a trace of mass was not entirely set in stone to be the best one in view of the discoveries. Warm effectiveness and NOx emanation were raised by 4.20 and 17.94%, respectively. The interest in the change had a restitution time of close to 62 days. This situation was picked when there is an extra limit on power creation, and the point is to lessen emanations however much could reasonably be expected.

Liu et al. (2017) [45] conducted a thorough investigation into modern low-emission combustion techniques employed in aero gas turbines. The researchers conducted an analysis of various technologies, specifically focusing on those with high-tech readiness levels. These technologies encompass rich-burn quick-quench lean-burn, double annular combustors, twin annular premixed swirler combustors, and lean direct injection. Additionally, they also considered emerging technologies that are currently at lower TRL levels.

Taamallah et al. (2015)[9] looked at the effects of fuel synthesis on premixed gas turbine ignition, with an emphasis on framework security and discharges, for blends of engineered gas (syngas) that are high in hydrogen. Syngas is basically comprised of H₂, CO, and CH₄, and its composition might change because of variations in the process's boundaries. These non-standard powers give various troubles in premixed ignition due to the altogether varying compound, transport, and warm qualities that set the syngas parts apart. A survey of current innovation that can deal with syngas and other hydrogen-rich powers is given, considering the difficulties associated with utilizing these energizers in genuine, enormous-scope business applications. Huge Whirlpool Recreations (LES) are at the front, splitting the difference between exactness and computational expense; however, there is equivalently little data on the premixed LES ignition of these powers. There is a requirement for more noteworthy concentration around here to help with beating the troubles given by these energizers.

Kumari and Sanjay (2015) [5] thanked about the thermodynamic and outflow execution of the BGT (essential gas turbine) and IcGT (intercooled gas turbine) cycles, including blower pressure proportion, TRIT (turbine rotor delta temperature), combustor-essential zone temperature, identicalness proportion, and home time. Thermodynamic investigation of the

recommended cycles uncovers that the IcGT cycle has a sensible proficiency that is 8.39% more noteworthy than the BGT cycle and has a generally high energy debasement rate that is 4.42% lower than the BGT cycle. As per outflow evaluation, NOx discharge is more noteworthy for the two cycles at higher upsides of r_p and c , while CO (carbon monoxide) emanation lessens with an expansion in equality proportion. The IcGT cycle's expanded UHC outflow is brought about by a cooler compressor input air temperature. Generally, IcGT cycle execution is better by and large.

Ditaranto et al. (2015) [46] studied an extraordinary gas turbine cycle thought might be utilized in power plants with coordinated gasification consolidated cycles (IGCC) or pre-burning CO₂ assortment to forestall fuel weakening and lessen NOx discharges. A high fume gas distribution (EGR) rate is utilized to deliver an oxygen-drained working liquid that enters the burning chamber, which is adequate to bring down the high reactivity of hydrogen-rich fills and keep a low pace of NOx age. A mathematical assessment of soundness and the potential for NOx emanations is utilized to create a first-request assessment of the burning qualities under these gas turbines working conditions. It is shown that fire strength might be kept up at EGR rates far higher than the most extreme EGR limit seen in customary flammable gas-terminated gas turbines, and huge decreases in NOx discharges are expected at these high EGR rates. This first-request investigation's decision is that there is a genuine chance to diminish the proficiency punishment welcomed by fuel weakening.

Najafi et al. (2014) [47] contemplated a thermodynamic, money-related, and natural (releases cost) showing of areas of strength for an influence module gas turbine (SOFC-GT) blend system joined with a multi-stage streak (MSF) desalination unit in their continuous work. A multi-objective inherited estimation (MOGA) is used to choose the plant's ideal arrangement limits. The smoothing-out approach achieves an energetic efficiency of 46.7% and a full-scale cost of \$3.76 million USD per year. The picked plan's remuneration time period is surveyed to be 9 years. This planned advancement is supposed to ensure success in the near future as SOFC capital costs are falling and their practical lifetimes are rising.

Memon et al. (2013) [48] investigated the thermo-ecological, financial, and relapse assessments of clear and regenerative gas turbine cycles. A parametric report is led to investigate the impacts of blower delta temperatures, turbine bay temperature, and blower pressure proportion on the boundaries of action cycles' exhibition, natural effect, and

expenses. Different polynomial relapse (MPR) models are made to interface huge reaction factors with indicator factors, and enhancement is completed to get the most ideal working circumstances. The functional boundaries fundamentally influence the exhibition boundaries, the climate, and expenses, and the burning chamber and exhaust stack are two huge places where the best exergy obliteration and misfortunes occur. The recovery cycle had a considerably lower and large exergy obliteration rate, which prompted a superior exergy productivity of the cycle. MPR models are dependable assessors of the reaction factors, and the best working boundaries are found utilizing these models, which improve cycle execution while bringing down CO₂ discharges and costs.

Elkady et al. (2011) [49] determined the lower limit of NO_x and CO emissions, as well as an emissions benchmark for practical gas turbine combustors, using a research burner and a chemical reactor model. A number of current kinetic processes were examined and compared, and sensitivity analysis was carried out to pinpoint significant responses. Coating steam turbine blades with nanomaterials is being studied to mitigate the potential detrimental impact of the corrosion process on emissions [50].

Ahmadi et al. (2011) [51] investigated a broad thermodynamic model of a trigeneration framework that produces power, intensity, and cooling. Boundaries that measure ecological impact and supportability are surveyed, alongside energy and exergy assessments, natural effect evaluations, and related parametric examinations. Results show that the framework has a more noteworthy energy productivity than standard joined intensity and power frameworks or gas turbine cycles, and its carbon dioxide emanations are lower than those of the correlation frameworks. The framework's energy productivity and natural impact are exceptionally influenced by the blower pressure proportion, gas turbine input temperature, isentropic effectiveness, heat recuperation steam generator strain, and blower pressure proportion. The ignition chamber has the highest exergy obliteration of all framework parts because of the enormous temperature contrast between the functioning liquid and the fire temperature. Bringing down the mass stream rate by means of the ignition chamber and expanding the turbine admission temperature might bring down natural effect costs.

2.4 THERMAL EFFICIENCY

Zoghi et al. (2021b) [23] examined the goal of this investigation, which is to recover waste intensity from a recuperation gas turbine cycle (GTC) when it is energized by a cross-variety heat source containing biomass gasification and a sun-situated power tower (SPT). The system uses a family bubbling water heat exchanger (DWHX), a LiCl-H₂O maintenance refrigeration structure (ARS), a steam Rankine cycle (SRC), and a thermoelectric generator (TEG) rather than a regular condenser to recover the waste energy of a GTC. With a multi-age energy efficiency of 43.11 percent, the proposed structure can generate 98.2 MW of force in the fundamental circumstances, with 24.7 MW of the outcome coming from waste intensity recovery from GTC in the SRC. The overall energy capability is upheld by 9.04 rate centres on account of GTC's waste force recovery. The proposed system's general cost rate is 7799 \$/h, and the multi-generational unit cost is 8.26 \$/GJ. The structure's thermodynamic capability declines with an extension in DNI, but it performs better concerning the economy and the environment. The warming creation rate lessens as the GTC blower's strain extent rises, and the structure's show encounters a monetary and regular viewpoint. The net power yield and multigenerational energy viability show up at their most outrageous levels at pressure extents of 14.6 and 11.2, independently. The age speed of power from a force recovery steam generator (HRSG) should be remarkably extended by raising the press temperature differential.

Koç et al. (2020) [26] dissected the power creation, heat, and energy efficiencies of clear and recuperative gas turbine cycles at reliable power yield (50 MW) and turbine outlet temperature (450 °C). The structure was dissected for the use of pure hydrogen and vaporous petroleum as fuel. Examination uncovered that, up to 18 bar pressure, the recuperative cycle's adequacy was more imperative than that of the fundamental gas turbine cycle. The usage of hydrogen in gas turbine cycles gives benefits over petrol gas in regard to execution, the environment, and CO₂ transmission, in spite of the fact that it costs more per unit of power. The base fuel costs were figured as 0.345 and 0.075 \$/kWh at 20 bars for clear gas turbine cycles, independently. The 50 MW gas turbine's CO₂ outpourings for petrol gas were found to go from 46.27 to 71.15 tons of CO₂/h.

Khan and Tlili (2019) [32] compared the energy and exergy investigation of gas turbine power plants is the subject of this examination. Exergy investigation is like energy

examination but incorporates subjective examination, while energy investigation is more quantitative. The thermodynamics' first and second regulations are utilized to develop the model for the gas turbine power plant. The energy and energy proficiency of the air blower are 94.9 and 92 percent, respectively, while the gas turbine has 92% of energy and 82 percent of energy productivity. The plant's all-out proficiency is 32.4 percent, and its energy and efficiency productivity are 34.3 percent. Decreased consumption air temperature further developed air-fuel proportion in the ignition chamber, and expanded gas turbine admission temperature resistance are important to streamline proficiency.

Soltani et al. (2013) [52] describe a fuelled gas turbine combined cycle coupled with a biomass gasification facility using energy and exergy techniques. The system's total energy efficiency is shown to reach a maximum at a certain pressure ratio, depending on the difference between the cold-end temperature of the heat exchanger and the gas turbine's input temperature. The rate of air flow decreases as the pressure ratio rises, whereas the rate of steam flow increases. To determine component ratings and biomass feed rates, the performance of a 1 MW plant is examined using a variety of operational settings. The main thermodynamic irreversibility's are also investigated, along with the energy efficacy of cycle components.

Zabihian and Fung (2013) [53] analysed the hybrid solid oxide fuel cell (SOFC) and gas turbine (GT) model to examine the impact of the type and content of the intake fuel on the cycle's performance. This study is essential for the hybrid SOFC-GT system's real-world use of made fuels, as few studies on the use of unconventional fuels have been published in the open literature. Simulation results for various input fuel types demonstrate how changes in the fuel type have a significant impact on system outputs and operating parameters. Before using biogas, gasifier biomass, and syngas as fuel, the potential of changing the incoming fuel type should be considered, and its effects should be examined.

Santos et al. (2016) [54] investigated how a thermodynamic model is utilized to gauge the presentation details of a sun-oriented mixture gas turbine power plant with inconsistent irradiance and surrounding temperature conditions. At the point when sun-powered illumination is sufficiently high, the model considers a sequential sun-oriented hybridization. The warm efficiencies of the connected subsystems and the vital intensity exchangers are joined to frame the general plant's warm productivity. Mathematical information for the

model's feedback boundaries was gotten from a recently developed focal pinnacle establishment in Seville, Spain. The bends for various factors, including general plant proficiency, sun-oriented subsystem effectiveness, sun-based share, fuel change rate, and power creation, are determined for commonplace days over time. Accepting flammable gas filling, fuel utilization is registered, and the decline in ozone-harming substance outflows is portrayed. The model can be utilized to figure out the day-to-day and occasional improvement of the presentation of real establishments.

Hou et al. (2017) [55] consolidated cycle connecting supercritical CO₂ recompression and recovery cycles is created to recuperate heat from marine gas turbine fumes and increment transport part-load warm proficiency. The cycle attributes have been inspected and changed, including yield power, energy productivity, heat exchanger region per unit power yield (APR), and leveled energy cost (LEC). The hereditary calculation-based multi-objective advancement approach is picked as the enhancement strategy to track down the best framework boundary. The proposed cycle is better than the normal, normal, and consolidated cycles and can give 80% of the boat's drive power in case of a gas turbine disappointment. It has the advantages of profound waste intensity usage, high conservativeness, and modest expense, making it ideal for maritime gas turbine squander heat recuperation.

Wang et al. (2020) [56] introduced a clever trigeneration system that involved a gas turbine cycle (GTC), a regenerative supercritical carbon dioxide (sCO₂) Brayton cycle, a characteristic Rankine cycle (ORC), and a maintenance refrigeration cycle (Bend). The sCO₂ cycle holds the waste power conveyed by the GTC before using it to fuel the ORC, while the coating curve is constrained by the leftover force to offer a cooling limit. An overall investigation is directed to assess the impact of ORC with various working fluids on the efficiency of the whole system. The structure can make 40.65 MW of net power, 6.02 MW of cooling limit, and 9.93 MW of warming weights, with a for the most part Exergoeconomic variable of 20.17%. The subsystem GTC takes everything into account, including destruction and the most essential complete capital cost. The part-consuming chamber has the highest exergy destruction rate, and the total unit costs for the fluids I-butane, n-pentane, and I-pentane events, independently, climb conversely, with the structure utilizing n-butane case by 0.27 percent, 1.09 percent, and 0.06 percent, respectively. The warm efficiency fell by 0.48 percent, 0.71 percent, and 1.20 percent, and the exercise efficiencies did as well.

Sayyaadi and Mehrabipour (2012) [57] investigated Proficiency improvement is being examined for a gas turbine cycle utilizing a Siemens gas turbine type V93.1 with a 60 MW ostensible result and 26.0 percent warm productivity. To increase warm effectiveness, a regular rounded vertical recuperative intensity exchanger is planned to be incorporated into the cycle as an air pre-radiator. A multi-objective streamlining method is utilized to determine the warm and mathematical necessities of the recovery and boost the exergetic effectiveness of the gas cycle. The NSGA-II strategy is utilized for streamlining programming, and Pareto ideal boondocks are found for the least, normal, and most extreme surrounding air temperatures in three situations. The Bellman-Zadeh, LINMAP, and TOPSIS procedures were utilized to pick the most definitive and fitting response in every situation. It has been shown that the TOPSIS and LINMAP leaders perform best when utilized at the normal encompassing air temperature.

Shirazi et al. (2014) [58] conducted an investigation and developed a mathematical framework for an ITES system. The purpose of this system was to cool the intake air of a gas turbine. The researchers then proceeded to evaluate the model from thermal, economic, and environmental perspectives. The study employed a multi-objective algorithm based on evolution to optimize the design parameters of the plant, taking into consideration the conflicting thermodynamic and economic objectives.

Dybe et al. (2021) [59] called it Top Cycle, which offers the required infrastructure for combustion to function on a range of fuels in a steam-rich environment. Electric efficiencies greater than 50% and power densities greater than 2100 kW/kg air are obtained while operating at design conditions (referred to as intake air flow). The cycle performance is identified via a sensitivity study as a function of representative factors, which serves as the foundation for future operation and design advancements. Maximizing the economizer heat recovery, raising the working pressure, and raising the turbine intake temperature are all efficient ways to increase Top Cycle's electric efficiency. The performance of Top Cycle is then contrasted with that of a cutting-edge combined cycle (CC) under identical operating conditions, resulting in a smaller plant footprint and dimensions and cheaper investment costs at the same power output.

Cho et al. (2015) [60] researched the supercritical CO₂ (S-CO₂) power cycle, which has drawn interest as a potential future power cycle innovation because of its small size and

warm productivity at generally low turbine consumption temperatures (450–750 °C). The review group accumulated various S-CO₂ cycle designs and assessed every one's exhibition with the end goal of improving the current situation with the innovation. Seven cycle setups were at last picked as a lining power framework, and the organization of each cycle was surveyed while the base strain, split stream rate, and mass stream rate were changed. The investigation discovered that the reference steam cycle performed better compared to the organization's proposal to join two S-CO₂ cycles, while the modern single cycle known as the fountain S-CO₂ Brayton cycle 3 was the main one to outflank the standard steam cycle. This finding delineates the potential for the S-CO₂ lining cycle if part advances advance to where they can uphold the presumptions made in this article.

2.5 MASS AND HEAT RECIRCULATION'S STRATEGIES

Mohammadpour et al. (2021) [61] surveyed the thermodynamic productivity of an oxy-biogas regenerative gas turbine cycle with CO₂ distribution. The principal and weakening zones are isolated in the CO₂ stream, and compound harmony demonstration is utilized for exercise examination in the fundamental zone. The net created power, the warm proficiency, the particular fuel utilization SFC, and the CO₂ catching mass stream rate are examined. The CO₂-to-O₂ molar proportion CT) in the essential zone and the essential diluent proportion PDR in the weakening zone have the most elevated upsides of warm proficiency, and by expanding CtO, energy annihilation diminishes in the two zones. Warm proficiency is raised by 9.92 percent when CtO is expanded in the range of 1.5–2.98, though warm productivity is diminished by 1.3%. SFC should be somewhere around 388 g/kWh in the PDR range, and it should be 387.4 g/kgWh in the CtO range. The turbine admission temperature might be appropriately controlled by utilizing the two-zone idea.

Ditaranto et al. (2020) [62] investigated the use of high hydrogen fuels in IGCC plants and gas turbines for the production of electricity with CO₂ capture or with hydrogen from renewable sources. The engine is operated at a high exhaust gas recirculation EGR rate to produce oxygen-depleted air, maintaining low NO_x emissions without the need for dangerous premixing or dilution. Results for both dry and wet EGR alternatives are shown in relation to the EGR rate. Nitrogen dilution has an efficiency cost of 1.3 percent, making it the optimum alternative even though all EGR solutions give an improvement. The efficiency improvement over the reference situation is 1%.

Bellas et al. (2019) [63] investigated Particular fume gas distribution (S-EGR) has been proposed to build the CO₂ convergence of vent gases from gas-terminated frameworks, empowering coordinated post-burning CO₂ extraction. This study evaluated the viability of a miniature gas turbine in mimicked S-EGR situations. At power results of 100 and 60 kW, most extreme pipe gas CO₂ convergences of 8.4 and 10.1 vol percent were accomplished, addressing a 4–7-fold expansion in CO₂ content over pattern circumstances. Influences on the framework's working execution and changes in CO, unburned hydrocarbon, and nitrogen oxide (NO_x) emanation patterns were assessed. Electrical proficiency diminished a smidgen, and emanations of unburned and halfway oxidized species expanded, especially at lower loads where fragmented ignition impacts were more articulated. NO_x discharges were lower because of lower fire temperatures, which brought about a less warm NO_x age.

Herraiz et al. (2018) [17] investigated Particular Fumes Gas Distribution (SEGR), an idea where CO₂ is explicitly reused to further develop fixation and decline pipe gas stream rates. It is utilized in equal or in series with a downstream PCC framework to raise CO₂ focus north of 14 vol percent and keep up with oxygen levels in the combustor at around 19 vol percent. This results in an improvement in net power creation of 42 MW (5.2%) and 18 MW (2.3%), as well as in net warm effectiveness of 0.55 percent and 0.83 percent, respectively. The utilization of 30 wt percent watery monoethanolamide for cleaning in SEGR brings about functional and monetary benefits. CO₂ selectivity, pressure drop, and intensity move stream rate are significant variables when picking an innovation for SEGR applications.

Hasemann et al. (2017) [64] investigated whether microgas turbines (MGT) can increase efficiency by adding an external exhaust gas recirculation (EGR). EGR's effect on the working fluid's composition has an impact on how pollutants are produced during combustion. This research evaluated a single-stage FLOXR-based combustor for an MGT operating in the power range of 1-3 kWel when used with EGR. N₂, CO₂, and steam were diluted with 718 °C of warmed combustion air. Measurements of OH chemiluminescence and emissions were conducted using an exhaust gas probe. Results indicate that the tested combustor can operate steadily even at extremely low oxygen levels at the combustor input, but the range of operation under EGR circumstances is constrained. The models conducted are consistent with the observed rise in CO emissions.

Tahmasebzadehbaie and Sayyaadi (2016) [65] investigated a turbo-compressor model modified to increase thermal efficiency and decrease NOx emissions using a cross-flow plate-fin heat exchanger as an air pre-heater and direct recirculation of flue gases into the combustion chamber. A frontier of the best solution, known as the Pareto frontier, was produced in objective space by minimizing the payback period for the heat exchanger's capital investment and NOx emission and maximizing the gas cycle's energetic efficiency. Bellman-Zadeh, TOPSIS, and LINMAP approaches were used to choose the ultimate best answer. The greatest outcomes, in contrast to the basic cycle, were shown to result in a 34.7% decrease in NOx emissions and a 5.8% gain in energy efficiency.

Taimoor et al. (2016) [66] presented a unique change to the combined gas turbine cycle that boosts overall effectiveness while reducing the creation of acidic gases when they are captured and rejected from the stack. Using ASPEN HYSYS® v8.6, the adjustment is applied to a simulated General Electric 9HA.02 turbine, and the differences between simulated and actual gas turbine characteristics are constrained by applying efficiency and exhaust temperature limits. Efficiency increased by 0.77 percent, and acidic gases (exhaust) were significantly reduced. A novel control method is added to the suggested alteration to improve efficiency in part-load situations.

De Santis et al. (2016) [67] assessed the expected utilization of fume gas distribution (EGR) for post-ignition CO₂ assortment by mathematically looking at the impacts of CO₂ weakening on the exhibition of a modern miniature gas turbine combustor. Form heat transfer (CHT) and radiation impacts have been considered in the improvement of an exhaustive 3D model of the burning chamber, and a careful substance system has been utilized inside the structure of the fire-produced manifolds to model the ignition cycle. The mathematical outcomes show that EGR might be a functional method to raise the CO₂ grouping of dry low-emission (DLE) combustors' vent gas and work on the viability of carbon partition. The ignition proficiency might be kept up with under the expected EGR settings while accomplishing fewer NOx emanations on account of the lower temperature levels inside the burning chamber.

Ali et al. (2015) [68] investigated gas turbines as an efficient and secure choice for producing heat and electricity that is also ecologically friendly. This research examines the microgas turbine's exhaust gas recirculation (EGR) process modeling and its effect on performance.

The optimal location of the EGR at the compressor intake with partial condensation resulting in the CO₂ enhancement to 3.7 mol percent is the outcome of the performance study.

Ali et al. (2014) [69] examined the Turbel T100 tiny gas turbine and its modification with exhaust gas recirculation (EGR). The system is thermodynamically evaluated using a steady-state model, and the process simulation with EGR provides an insightful analysis. CO₂ is enriched as a consequence of the EGR model, which lowers the energy need of the CO₂ capture system.

Cameretti et al. (2013) [69] examined the use of liquid and gaseous biofuels in a micro-gas turbine. It tests the viability of strategies for providing the microturbine with fuels from sustainable sources as well as pollutant emission control. A revised main fuel injector form and placement for liquid fuel delivery are paired with a different pilot injector position, and an external EGR option is active in the event of biogas fueling. Both approaches use a flameless combustion concept-based approach to reduce heat and NO production.

Canepa et al. (2013) [70] used modeling and simulation to do a thermodynamic study of a combined cycle gas turbine power plant with post-combustion CO₂ collection. Aspen Plus and Gate Cycle were used to model the power plant and CO₂ collection facility. The CO₂ capture system was scaled up from a pilot plant to commercial size. Performance analysis was done using the integrated model. It has been suggested that exhaust gas recirculation may lower flue gas flow rates while increasing the CO₂ content of the flue gas. This could improve thermal efficiency without significantly altering the original power plant.

Belaissaoui et al. (2012) [71] investigated inside and out. Research is being finished on post-burning carbon catch and capacity (CCS) for coal power plants. This exploration covers the potential for carbon capture on a gas turbine utilizing a vent gas reusing and film partition blend. The energy necessities of the different cycles, addressed in GJ (warm premise) per ton of recuperated CO₂, and the size of the film catch process (communicated in m² of layer region) have been assessed. It is shown that under ideal working conditions, in view of oxygen-improved air (OEA) burning and an exceptionally specific film (CO₂/N₂ selectivity of 200), it very well might be feasible to decrease the complete energy interest down to 2.6 GJ per ton. Different choices are introduced to decrease the energy punishment of the cycle.

Sander et al. (2011) [72] inspected the impacts of FGR on the two gas turbines (GT) and joint cycle power plants (CCPP). FGR is the most common way of taking care of incompletely cooled vent gas from the HRSG back into the GT consumption, which can emphatically raise CO₂ focus, decline volumetric stream to the CO₂ catch unit, and work on generally speaking execution of the CCPP with CO₂ assortment. Prior to being blended in with the surrounding air, the part of pipe gas that is directed back to the GT must be additionally cooled. Pipe gas distribution proportion and temperature awareness tests are completed to gauge the adjustment of working liquid organization, the general dampness at the blower admission, and the impact on by-and-large execution on both GT and CCPP. The air/fuel proportion (AFR) for the burning framework is a vital measurement to show what FGR means for the ignition cycle. Furthermore, an activity idea for a GT with FGR is inspected.

Li et al. (2011) [73] found that increasing the CO₂ content of exhaust gases is a potentially efficient way to lessen the electrical efficiency of MEA-based chemical absorption. Quantitative research has shown that a recirculation ratio of 50% may raise the CO₂ concentration from 3.8 to 7.9 mol% and decrease the mass flow of the absorber feed stream by 51.0%. The reboilers overall thermal energy use has decreased by 8.1%. An optimal EGR ratio of roughly 50% may boost total NG LHV efficiency by 0.4 percentage points. Low oxygen concentrations may negatively affect the stability and completeness of combustion but may have a favourable impact on NO_x emission reductions and amine degradation.

Steinberg et al. (2010) [74] investigated a careful assessment of the stream fire communications related to acoustically related heat discharge rate varieties in a 10 kW CH₄/air Whirl-settled fire in a gas turbine model combustor shows self-energized thermo-acoustic motions at 308 Hz. Fast stereoscopic molecule picture velocimetry, gracious planar laser-produced fluorescence, and OH* chemiluminescence estimations at a supported reiteration pace of 5 kHz uncovered various concurrent intermittent movements utilizing transient legitimate symmetrical disintegration. At the thermo-acoustic recurrence, enormous motions in the fire surface region were seen, which significantly affected the general motions of intensity discharge. Enormous scope prolongation of the response layers achieved by the changing reactant stream rate was responsible for around half of the

varieties, while the excess half was split between a limited scope stochastic crease and a huge scope groove.

2.6 OBJECTIVE

The goal of studying a gas-turbine cycle's ecological outflow and warm effectiveness by mass and intensity distribution techniques is to find ways to make gas-turbine power plants less harmful to the environment while also making them more productive. This includes dissecting the discharges delivered by gas-turbine power plants and distinguishing ways of limiting them, as well as concentrating on the thermodynamics of the gas-turbine cycle to recognize open doors for working on its productivity. One way to deal with diminishing emanations from gas-turbine power plants is to recycle a portion of the fume gases once more into the ignition chamber, which can lessen how much nitrogen oxide (NOx) and carbon monoxide (CO) are delivered. Heat distribution, then again, includes catching waste intensity from the exhaust gases and utilizing it to preheat the burning air or to create steam for different purposes.

The general objective of these procedures is to increase the amount of energy separated from the fuel while at the same time decreasing the number of harmful discharges delivered into the air. Thusly, gas-turbine power plants can turn out to be all the more harmless to the ecosystem while likewise working on their general execution and effectiveness.

3. METHODOLOGY

3.1 INTRODUCTION

Using In this chapter, all the settings and equations used in the numerical aspect of the study will be reviewed, as will the properties of the thermal materials used in this study.

3.2 ANSYS PACKAGE

The field of liquid mechanics known as computational liquid elements (CFD) utilizes mathematical strategies and calculations to reproduce and look at the way liquids behave, including gases and fluids, in various actual frameworks. It has developed into a pivotal instrument for exploring and gauging liquid stream peculiarities in the fields of design, physical science, and different sciences. Principal ideas of liquid elements, for example, the Navier-Stirs-up conditions that make sense of the protection of mass, force, and energy in liquid streams, are at the groundwork of computational liquid elements (CFD). To appraise the liquid's conduct over the long run and space, CFD reenactments disintegrate complex liquid stream issues into discrete computational parts, for example, cells or framework focuses, and afterward settle these conditions iteratively.

In the ongoing review, air is considered the running liquid in the framework. The qualities of the stream are thought to be consistent, three-layered, Newtonian, incompressible, and tense.

3.3 GOVERNING EQUATIONS

3.3.1 Standard $k-\epsilon$ Model

TRNSYS The accompanying vehicle conditions are utilized to determine the motor energy of the choppiness, k , and its pace of dissemination [20]:

$$\frac{\partial}{\partial t}(\rho k) + \frac{\partial}{\partial x_i}(\rho k u_i) = \frac{\partial}{\partial x_j} \left[\left(\mu + \frac{\mu_t}{\sigma_k} \right) \frac{\partial k}{\partial x_j} \right] + G_k + G_b - \rho \epsilon - Y_M + S_k \quad (3.1)$$

And

$$\begin{aligned}
& \frac{\partial}{\partial t}(\rho \varepsilon) + \frac{\partial}{\partial x_i}(\rho \varepsilon u_i) \\
&= \frac{\partial}{\partial x_j} \left[\left(\mu + \frac{\mu_c}{\sigma_z} \right) \frac{\partial \varepsilon}{\partial x_j} \right] + C_{1z} \frac{\varepsilon}{k} (G_k + C_{3c} C_b) - C_{2z} \rho \frac{\varepsilon^2}{k} + S_s
\end{aligned} \tag{3.2}$$

G_k , not set in stone as per the directions in Displaying Tempestuous Creation in the k-e Models, signifies the production of choppiness motor energy coming about because of mean speed slopes. Impacts of Lightness on Choppiness in the k-e Models depicts how to compute G_b , which is the dynamic energy created by lightness that causes disturbance. As figured in Impacts of Compressibility on Disturbance in the k-e Models, Y_M the variable dilatation in compressible choppiness' commitment to the complete dissemination rate. Constants incorporate C_{1r} , C_{2r} and C_{32} . The violent Prandtl numbers for k and ε_r are σ_ε and σ_k , individually. Client- characterized source terms S_k and S_z are utilized.

Combining k and the turbulent (or eddy) viscosity μ_t is calculated as follows:

$$\mu_t = \rho C_\mu \frac{k^2}{\varepsilon} \tag{3.3}$$

where C_μ is a steady. The model constants $C_{1\varepsilon}$, $C_{2\varepsilon}$, C_μ , σ_k , and σ_ε have the accompanying default values: $C_{1\varepsilon} = 1.44$, $C_{2\varepsilon} = 1.92$, $C_\mu = 0.09$, $\sigma_k = 1.0$, $\sigma_\varepsilon = 1.3$.

These default values were laid out by concentrating on basic violent streams, including limit layers, blending layers, and planes—shear streams that are routinely experienced—as well as on rotting isotropic network disturbances. They have been found to work fairly well for an assortment of free and wall-limited shear streams. Although the model constants' default values are the laid-out industry norms, you can modify them (if important) in the Thick Model Discourse Box.

3.3.2 Mass Equation

The commitment to the mass hotspot for ease p in a cell is [20].

$$m_p = -m_{pq'} \tag{3.4}$$

3.3.3 Momentum Equation

There is no energy source. For the Eulerian model, the energy source in a cell for stage p is [20].

$$m_p \vec{u}_p = -m_{p i q} \vec{u}_p \quad (3.5)$$

And for phase q is

$$m_q \vec{u}_q = m_{p q q} \vec{u}_p \quad (3.6)$$

3.3.4 Energy Equation

For every single multiphase model, the accompanying energy sources are added. The energy source in a cell for stage p is [20].

$$H_p = -m_{p i q i} (h_q^{f^i} - h_p^{f^k}) \quad (3.7)$$

And for phase q is

$$H_q = m_{p i q' i} (h_q^{f^j} - h_p^{f^i}) \quad (3.8)$$

where $h_p^{f^i}$ and $h_q^{f^j}$ are the arrangement enthalpies of species i of stage p and species j of stage q, separately. The distinction between $h_p^{f'}$ and $h_q^{f'}$ is the dormant intensity.

3.4 SYSTEM GEOMETRY

The models were designed using the Solid Work program, version 2022. SolidWorks is 3D computer-aided design (CAD) software used for creating models and designs for mechanical, electrical, and architectural engineering projects. It allows designers and engineers to create detailed 3D models, simulate movement and performance, and generate technical documentation for production. SolidWorks is widely used in industries such as aerospace, automotive, Defense, and manufacturing. Its features include sketching, 3D modeling, assembly design, sheet metal design, and rendering.

Where the shell and tube type heat exchanger were designed to suit the function of the simulation work as shown in Figure 3.1, the intermediate barriers were changed in several possibilities, once when the intermediate barriers were 6, 8 times, and 10 times, as well as two types of heat exchangers being used: a heat exchanger that works on 3 tubes and a heat exchanger that works on 5 tubes.

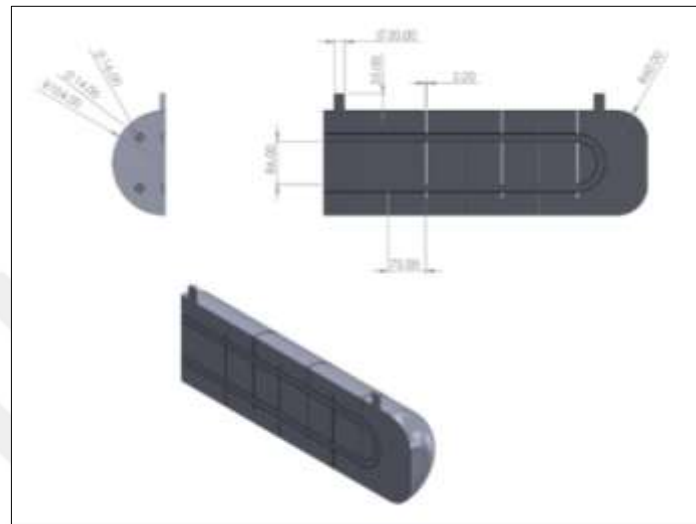


Figure 3.1: Shell and Tube Design.

3.5 MESH GENERATION

Generally, unstructured matrices are effective for complex calculations, so for the above reason, the unstructured tetrahedron frameworks were utilized in the ongoing review.

With just one phase from the user, ANSYS can generate solid geometry meshes and three-dimensional models. In this investigation, cells were extracted from a total of 2090107 tetrahedron elements, and the size of the element was 1 mm (see figure 3.2).

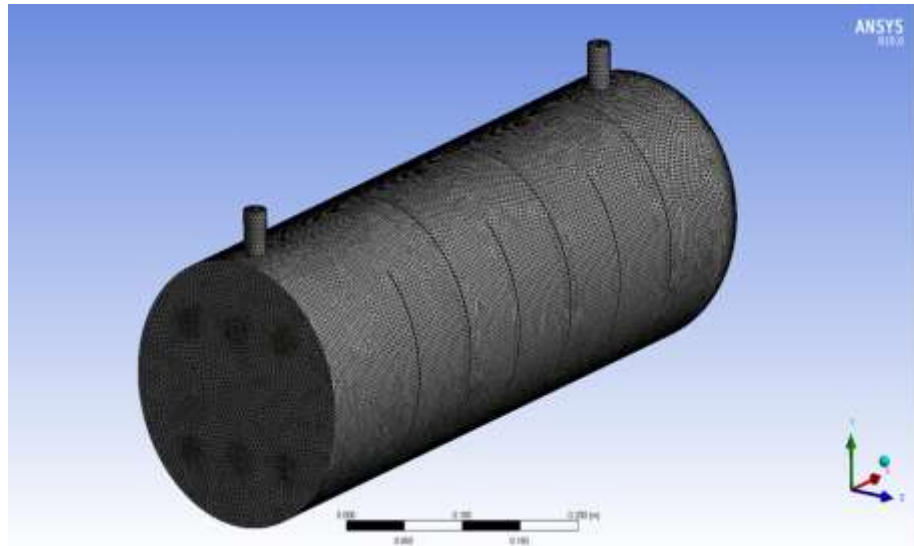


Figure 3.2: Mesh Generated.

An accurate network must be created to solve the equations because the simulation process depends on complicated algorithms to work on the matrices present in the domain. After that, use the mesh's dependability to find a remedy and bring the outcomes to a stable condition. It is important to create more than one network and more than one mesh dependability due to the variety of models that have been simulated. The value of the element was 2090107 when the outlet temperature in the cold tube reached 422.9 K, as shown in Table 3.1.

Table 3.1: Mesh Independency.

| Case | Element | Node | Outlet temperature in cold tube k |
|------|---------|--------|-----------------------------------|
| 1 | 845554 | 195655 | 428.6 |
| 2 | 1257856 | 305456 | 424.8 |
| 3 | 1643458 | 468030 | 423.2 |
| 4 | 2090107 | 553175 | 422.9 |

3.6 CONDITIONS OF THE BOUNDARY

The parameters of the heat exchanger input depend on the inputs of the EES program, which include the temperature difference across the compressor, which was taken as 745, 916, and 1055 degrees Celsius, as well as the pressure value, which represents 120 kPa and 100 kPa.

3.7 PROBLEM SOLUTION

The accompanying headways make up a part of the control-subordinate strategy that can be utilized for the plan:

- i. On the battleground, a lattice is made.
- ii. The blend of each control volume of the directing circumstances makes situations like speed, pressure, and safeguarded scalars that are logarithmic.

The discretized conditions are iteratively and directly tackled.

The game plan computation utilized by Familiar and consolidated in this work is in ANSYS. The administrative prerequisites are tended to consecutively (i.e., freely of each other). Since the overseeing conditions are backhanded (and coupled), it might take a few cycles to finish before a brought-together understanding is reached.

3.7.1 Solution Parameters

The arrangement boundaries incorporate the accuracy solver type. Normally, single- and two-fold tasks are utilized to track down exact solvers. In a PC with limitless exactness, residuals would disappear as the plan met up. A genuine PC, the extras rot to an insignificant worth ("change") and afterward quit modifying ("level out"). Also, Emphases Number is the most noteworthy digit of cycles done before the solver ends.

3.7.2 Convergence Criteria

The association of the fluid stream conditions up until it consolidates should be featured while utilizing the CFD strategy. At the point when the course of action stays within the exactness of the chosen mixing principles, the cycles reach a conclusion. The mistake residuals, which are the distinctions between the potential gains of a variable in two consecutive accentuations normalized by the greatest by and large leftover for the initial five cycles, are the procedure most often used to really take a look at plan mix. At the point when the residuals fall under a flexibility edge of 10⁻⁶ for all the fluid stream conditions depicted, the game plan is intended to be consolidated.

3.8 EES

The model considered in this paper is set up to look at the consistent case of the petroleum gas combined cycle. It is made up of a Brayton cycle, which includes an air blower (AC), a combustion chamber, and a gas turbine (GT). The following is a summary of the clamping frame's operating instructions. The air is warmed up and compressed to function tightly when it enters the air blower (AC). After that, the air is charged into the control chamber, where it reacts by releasing gaseous gasoline fuel to create high-pressure, high-temperature exhaust gases. The exhaust gases expand through GT to supply mechanical energy. By leveraging the temperature of the exhaust gases, HX transforms into steam in pressured water at high temperatures.

3.9 GENERAL MASS, ENERGY, AND EXERGY EQUATIONS

The preservation of mass conditions for the SSSF open framework [21]:

$$\sum \dot{m}_{in} = \sum \dot{m}_{out} \quad (3.9)$$

where: $\sum \dot{m}_{in}$ is the total mass flow entering per unit time, and $\sum \dot{m}_{out}$ the total mass flow exiting per unit time. The energy balance for every part depends on the primary law of thermodynamics for the SSSF open framework [21]:

$$\dot{Q} + \dot{W} = \sum \dot{m}_{out} h_{out} - \sum \dot{m}_{in} h_{in} \quad (3.10)$$

where: The amount of heat transmission per unit of time. \dot{W} Time spent working by the control volume, h_{in} : Specific enthalpies for each mass that enters the system and for each mass that leaves the system. Entropy is delivered due of irreversibility; hence it is not measured in open and closed frameworks like mass and energy are. The entropy equilibrium can be expressed as [21] in open frameworks:

$$\dot{E} = \dot{m}\psi \quad (3.11)$$

$$\psi = (h - h_0) - T_0(s - s_0) \quad (3.12)$$

Where s_0 : The mass's specific entropy as it enters the open system. s : The mass coming from the open system's specific entropy. T_0 : The temperature at which the open system and its surroundings meet. \dot{E} : The flow of energy, ψ The precise energy.

3.10 THERMODYNAMIC ANALYSIS FOR BC MODEL

Understanding and improving energy conversion processes depends heavily on thermodynamic analysis, and one of the key cycles examined in thermodynamics is the Brayton Cycle (BC). The thermodynamic cycle known as the Brayton Cycle is what drives the functioning of gas turbine engines, such as those seen in aircraft and numerous commercial gas turbines that produce electricity. The Brayton Cycle must be examined using thermodynamic concepts if these devices are to operate more effectively. The compression, combustion, expansion (which produces power), and exhaust processes are the four basic steps that make up the BC model, which is a condensed description of the gas turbine cycle. The BC model's thermodynamic analysis entails assessing numerous cycle parameters and performance measures using general concepts and equations. An essential resource for engineers and academics working on gas turbine engines and associated technologies is thermodynamic analysis for the Brayton Cycle (BC) model. Making educated design decisions and enhancing the performance of these systems to produce more power and higher efficiency is made easier by having a better understanding of the energy conversion processes within them.

3.10.1 Compressor Model

Air blowers are machines that utilize the ability to make dynamic energy, pack and compress air, and may, in short, explode. Rotating blowers are expected because of the huge stream speeds of turbines and their relatively low-pressure proportions. The fiber connection for the blower model is changed as follows [22]:

Air blowers are machines that utilize the ability to make dynamic energy, pack and compress air, and may, in short, explode. Rotating blowers are expected because of the huge stream speeds of turbines and their relatively low-pressure proportions. The fiber connection for the blower model is changed as follows [22]:

- Energy balance

$$\dot{W}_{AC} = \dot{m}_{\text{air}} (h_2 - h_1) \quad (3.13)$$

- Isentropic efficiency

$$\eta_{AC} = \frac{\dot{W}_{AC,S}}{\dot{W}_{AC}} \quad (3.14)$$

Exegetic relations for the blower model are altered as follows:

c. Exergy balance:

$$\dot{E}_{D,AC} = (\dot{E}_1 - \dot{E}_2) + \dot{W}_{AC} \quad (3.15)$$

d. Exergy efficiency:

$$P_{AC} = \dot{E}_2 - \dot{E}_1 \quad (3.16)$$

$$F_{AC} = \dot{W}_{AC} \quad (3.17)$$

$$\varepsilon_{AC} = \frac{P_{AC}}{F_{AC}} = 1 - \frac{\dot{E}_{D,AC}}{F_{AC}} \quad (3.18)$$

Where; P_{AC} is Product., F_{AC} Fuel , and ε_{AC} Exergy efficiency.

3.10.2 Combustion Chamber Model

The region of the gas turbine where energy is introduced is called the start chamber. The gas turbine cycle's wellspring of energy is the combustor. It attracts air, adds fuel, joins the two, and afterward permits the subsequent blend to be consumed. This philosophy is habitually completed under consistent pressure, regardless of whether just minor pressure issues are present much of the time. A critical quality of consumption is temperature, which is in many cases determined by the properties of the substance. The materials must be impervious to outrageous temperatures and temperature tendencies. Some other strategy could bring about the gas turbine missing the mark [22].

The energetic connection for the ignition chamber model is altered as follows:

a. Energy balance:

$$\dot{m}_2 h_2 + \eta_{CC} \dot{m}_3 LHV = \dot{m}_4 h_4 \quad (3.19)$$

The energetic relations for the ignition chamber model are changed as follows:

b. Exergy balance:

$$\dot{E}_{D,CC} = \dot{E}_2 + \dot{E}_3 - \dot{E}_4 \quad (3.20)$$

c. Exergy efficiency:

$$P_{CC} = \dot{E}_4 \quad (3.21)$$

$$F_{CC} = \dot{E}_2 + \dot{E}_3 \quad (3.22)$$

$$\varepsilon_{CC} = \frac{P_{CC}}{F_{CC}} = 1 - \frac{\dot{E}_{D,CC}}{F_{CC}} \quad (3.23)$$

3.10.3 Gas turbine Model

All gas turbines are planned as a joined conduit, where vaporous energy isn't provided nor eliminated, but rather changed from strain and temperature to speed. As air moves from a major admission to a more modest leave, the speed of the air increases. At higher velocities, pressure rises. The general tension in the framework stays consistent, and since no energy is provided or removed, static strain drops. This might be seen as static tension being changed over completely to affect pressure, with the end goal being that an expansion in static strain is joined by a progression of air by means of a united pipe and extension. Any development brings about a comparing temperature decline [22].

The energetic connection for the gas turbine model is altered as follows:

a. Energy balance:

$$\dot{W}_{GT} = \dot{m}_{gas}(h_4 - h_5) \quad (3.24)$$

b. Isentropic efficiency:

$$\eta_{GT} = \frac{\dot{W}_{GT,s}}{\dot{W}_{GT}} \quad (3.25)$$

Exergetic relations for the gas turbine model are altered as follows:

c. Exergy balance:

$$\dot{E}_{D,GT} = (\dot{E}_4 - \dot{E}_5) - \dot{W}_{GT} \quad (3.26)$$

d. Exergy efficiency

$$P_{GT} = \dot{W}_{GT} \quad (3.27)$$

$$F_{GT} = \dot{E}_4 - \dot{E}_5 \quad (3.28)$$

$$\varepsilon_{GT} = \frac{P_{GT}}{F_{GT}} = 1 - \frac{\dot{E}_{D,GT}}{F_{GT}} \quad (3.29)$$

3.11 ECONOMIC ANALYSIS

The main costs of a warm structure are the capital endeavor, the action and upkeep, and the fuel costs. Considering the capital recovery factor (CRF), a superior monetary model can be applied. The total capital endeavor (TCI) in a plant is given by how much all the purchased gear costs (PEC) are copied by a consistent part. The hard and fast capital interest in a plant is given in this way by [22]:

$$\dot{Z}_k = \frac{Z_k \times CRF \times \phi}{N \times 3600} \quad (3.30)$$

Where: *PEC*: the hardware's buy cost in US dollar. ϕ : the support factor (1.06). CRF: the Capital Recuperation Element, which can be determined as:

$$CRF = \frac{i(1+i)^n}{(1+i)^n - 1} \quad (3.31)$$

Where *I*: the loan cost (viewed as 10%); *n*: the lifetime of the framework (viewed as 20 years). The purchase gear cost (PEC) for the NGCC parts is according to the accompanying: Brayton cycle gear buy costs [22]:

a. Air compressor

$$ZAC = (71.1m40.9 - \eta_{AC})(P5P4) \ln(P5P4) \quad (3.32)$$

b. Combustion chamber

$$ZCC = (46.08m40.995 - P7P5)(1 + \exp - (0.018T7 - 26.4)) \quad (3.33)$$

c. Gas turbine

$$ZGT = (479.34m70.92 - \eta T) \ln (P7P8)(1 + \exp - (0.036T7 - 54.4)) \quad (3.34)$$

d. Steam turbine

$$ZST = 6000(WST)0.7 \quad (3.35)$$

3.12 COST PERFORMANCE

The framework all-out cost rate, barring fuel costs (\dot{Z}), is the summation over all parts of the following condition [22]:

$$\dot{Z}_T = \sum_k \dot{Z}_k = \sum_k (\dot{Z}_k^N + \dot{Z}_k^{OM}) = \frac{\sum_k CRF \beta (1 + \gamma) PEC_k}{\tau} \quad (3.36)$$

3.13 SUPPOSITIONS AND INFORMATION BOUNDARY TO THE CONSOLIDATED FRAMEWORK

The general assumptions made for the diversion of the joined structure are recorded as follows: All pieces of the joined system work under predictable state conditions; the synthesis of air at the channel of AC is 79% N₂ and 21% O₂; petroleum gas is completely oxidized in the CC; and ideal gas guidelines apply to the vapor gases. Furthermore, the CC is safeguarded completely. The information for the NGCC examination is listed in Table 3.2.

Table 3.2: Operation Condition Used for the AC [23].

| Parameter | Value |
|---------------------------------------|-------|
| Compression ratio | 12 |
| Mass flow rate of fuel, kg/s | 2.4 |
| Mass flow rate of exhaust gases, kg/s | 145 |
| Exhaust gases temperature, K | 400 |
| Ambient temperature, K | 288 |
| Turbine efficiency, % | 90 |
| Compressor efficiency, % | 86 |
| Pump efficiency, % | 85 |

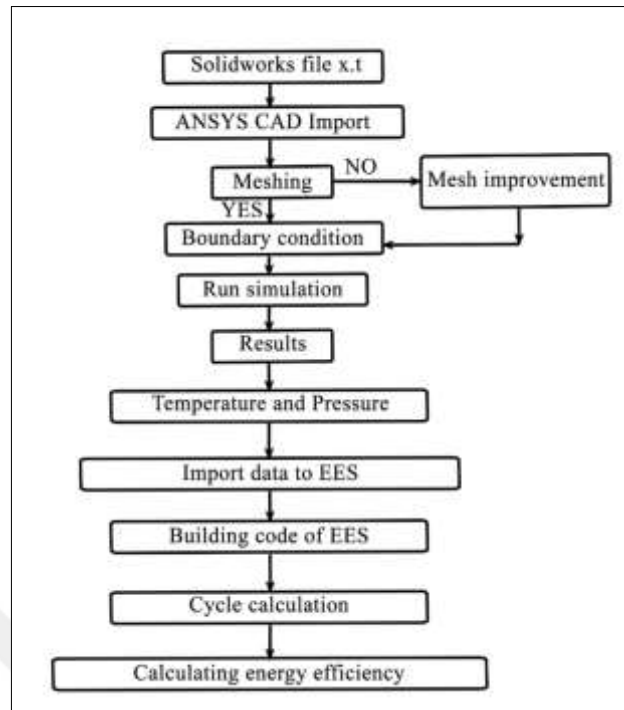


Figure 3.3: Flow Chart.

4. RESULTS AND DISCUSSIONS

4.1 INTRODUCTION

In this chapter, we will discuss the results produced by the tests, where 3 and 5 heat exchanger pipes were taken separately at three temperature degrees with two pressures as shown in Table 4.1 to see the overall energy, energy, electricity, and net work of the system. The ANSYS program will design the heat exchanger, and the results that are extracted will be transferred to the EES program to study the cycle.

Table 4.1: Study Cases.

| Name | Case 1 | Case 2 | Case 3 |
|----------------------------|--------|--------|--------|
| Effect of baffles | 6 | 8 | 10 |
| Effect of pipes | 3 | 5 | |
| Effect of temperature (°C) | 745 | 916 | 1055 |
| Effect of pressure (kpa) | 100 | 120 | |

4.2 EFFECT OF BAFFLES

Baffles provide several benefits when used in heat exchangers. Baffles make the fluid flow more turbulent, which accelerates the rate of heat transfer. Baffles, which control fluid flow, help avoid the development of stagnant zones, which may cause fouling and reduce the heat exchanger's efficiency. Additionally, baffles support the tubes structurally and assist in reducing vibration and damage. Where flow-induced vibrations occur during certain processes, the support intervals may be shorter. By guiding the flow through the shell in a certain direction, baffles support the tubes and help avoid mechanical vibrations that may cause the tubes to contact, leading to leaks and failures, especially close to the tube sheets. Additionally, by doing this, the heat exchanger's stagnant pockets are reduced, and turbulence is increased. By adding baffles, we can also keep the target velocity constant. In this study, the main three baffles (6, 8, and 10) were taken in simulations for temperature, pressure, and velocity to explain the behavior of the parameters as shown in Figure 4.1.

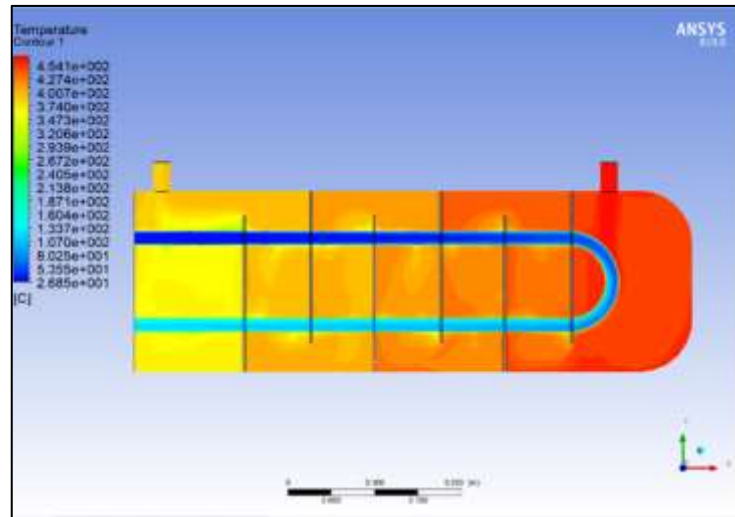


Figure 4.1: Temperature at 6 Baffles.

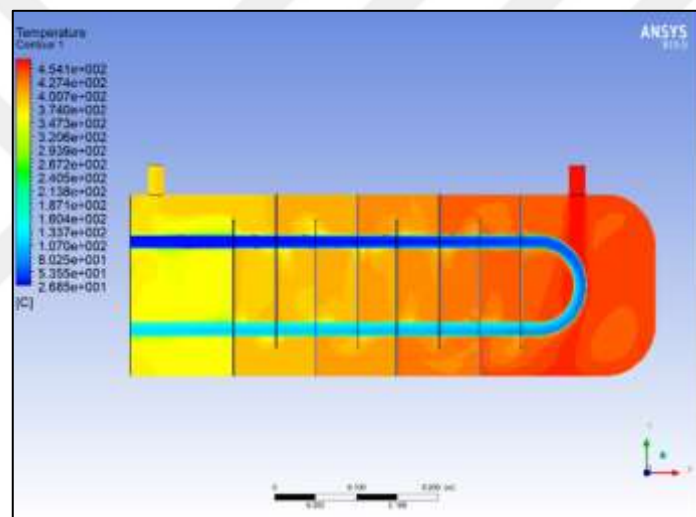


Figure 4.2: Temperature at 8 Baffles.

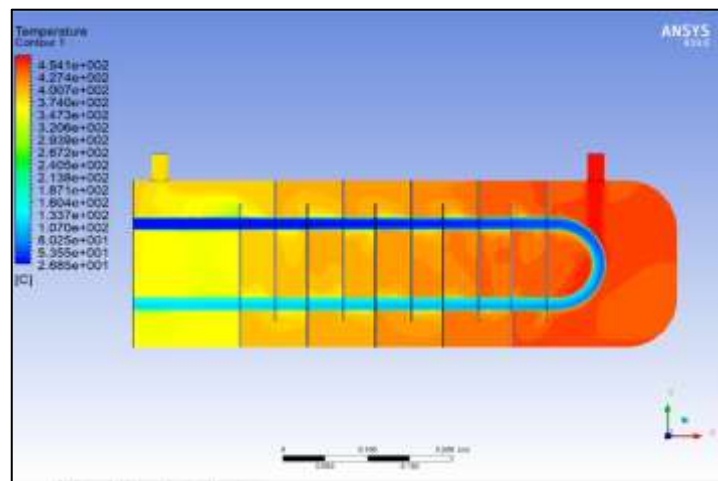


Figure 4.3: Temperature at 10 Baffles.

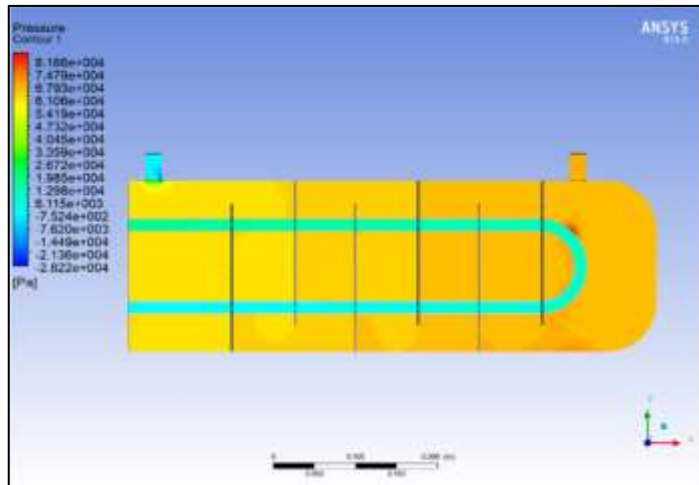


Figure 4.4: Pressure at 6 Baffles.

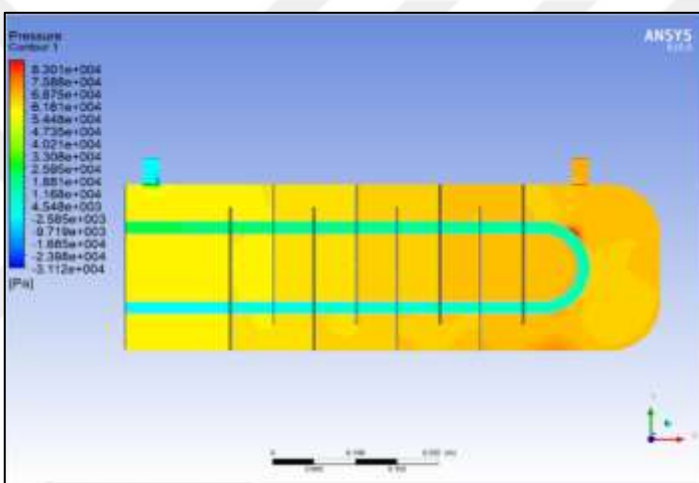


Figure 4.5: Pressure at 8 Baffles.

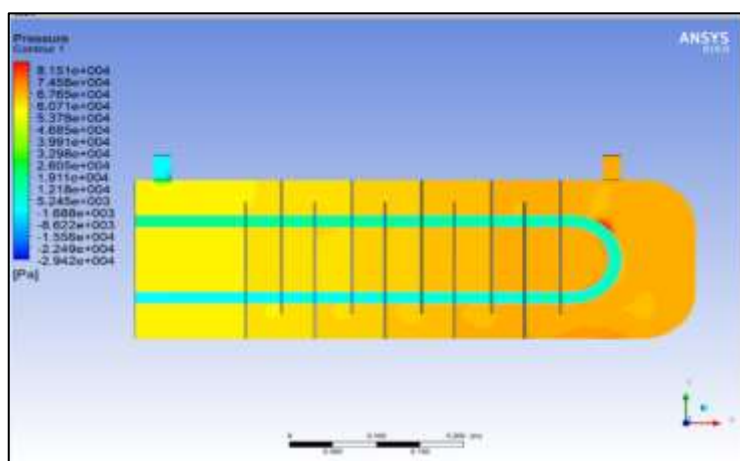


Figure 4.6: Pressure at 10 Baffles.

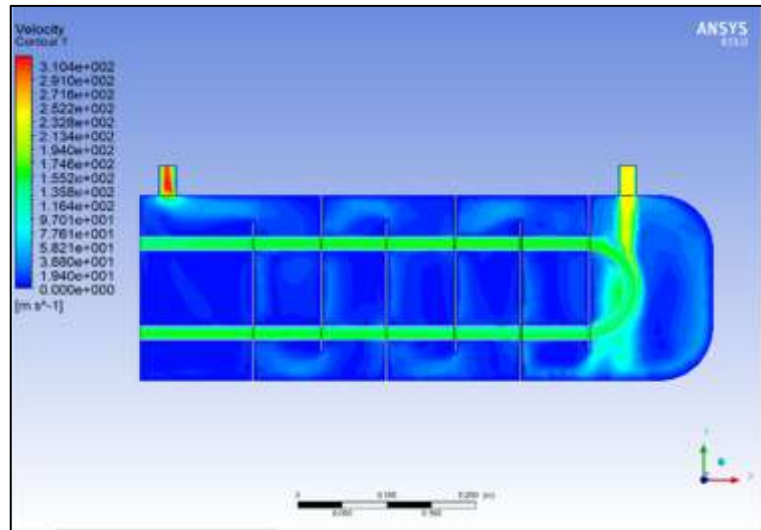


Figure 4.7:Velocity at 6 Baffles.

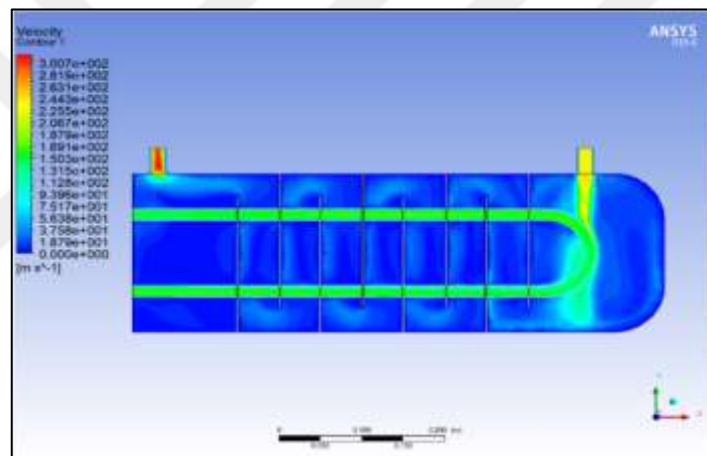


Figure 4.8:Velocity at 8 Baffles.

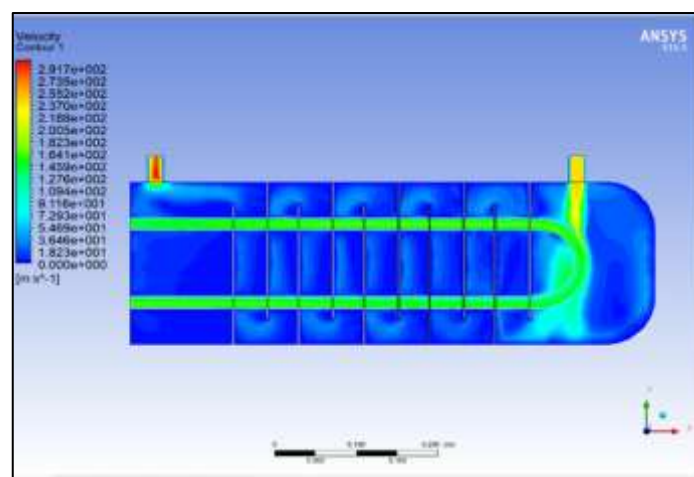


Figure 4.9:Velocity at 10 Baffles.

According to the investigation, adding more baffles increases the pressure drop and heat transfer rate of the system, but at large numbers of baffles, the pressure decreases because it prevents the flow of fluid and decreases its velocity, but the temperature increases because of the long path inside the pipes and the non-straight path, which makes the fluid take more time through the pipes.

4.3 EFFECT OF PIPES

In recent times, advancements in the field of control theory and information technology have played a pivotal role in enhancing the effectiveness of thermal control systems. Numerous approaches have been undertaken in order to enhance heat transfer and achieve greater efficiency in the production of heat exchangers. The current multi-pipe heat exchanger has superior performance compared to the twin-centric tube heat exchanger. The utilization of multi-pipes has several benefits, including an increased surface area for heat transmission per unit length and an enhanced overall heat transfer coefficient. Furthermore, enhancements were made to the thermal interaction between the fluids. The use of these specific heat exchangers offers technical and economic benefits as a result of their capacity to facilitate heat transfer among three fluids within a singular apparatus. This study aimed to investigate the impact of varying the number of pipes on the parameters of a heat exchanger. To do this, three and five pipes were selected as the experimental conditions for analysis see Figure 4.2.

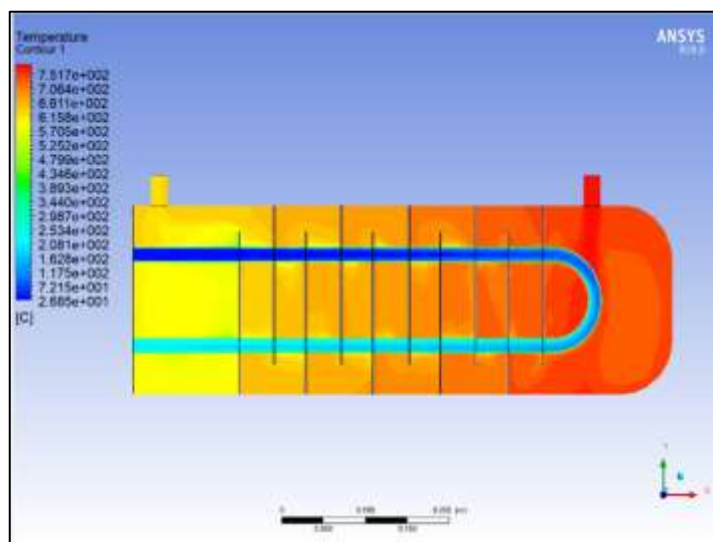


Figure 4.10: Temperature at 3 Pipes.

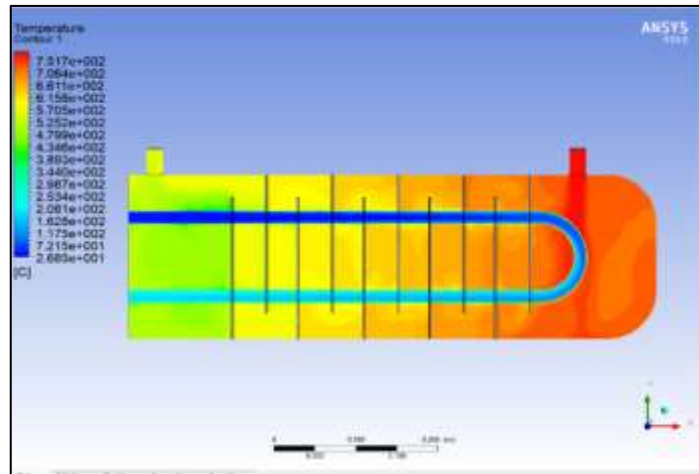


Figure 4.11: Temperature at 5 Pipes.

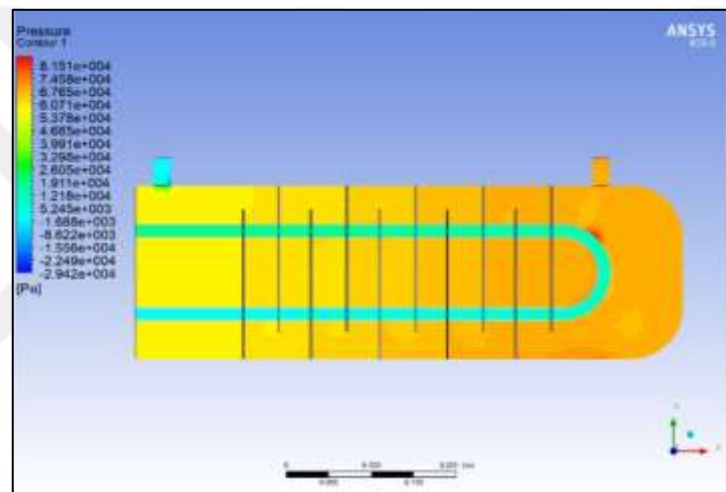


Figure 4.12: Pressure at 3 Pipes.

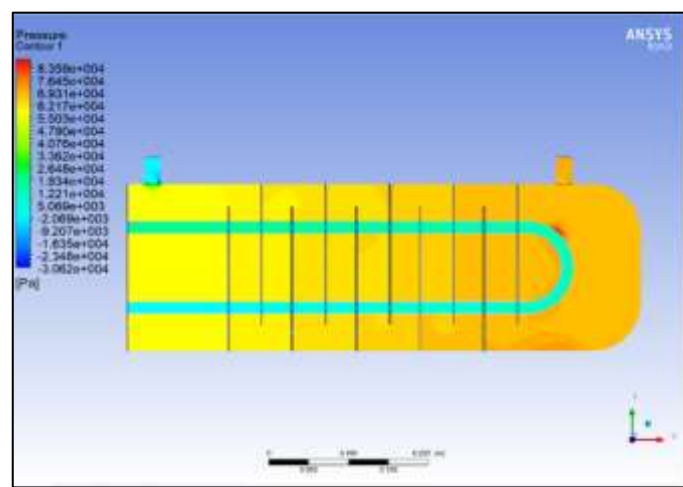


Figure 4.13: Pressure at 5 Pipes.

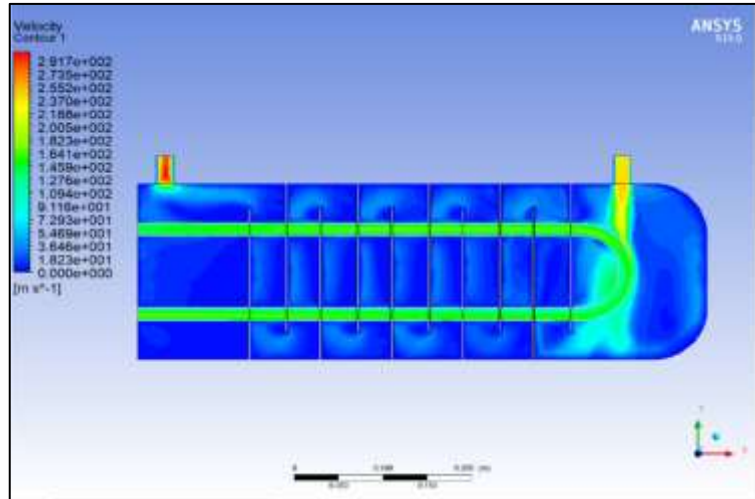


Figure 4.14: Velocity at 3 Pipes.

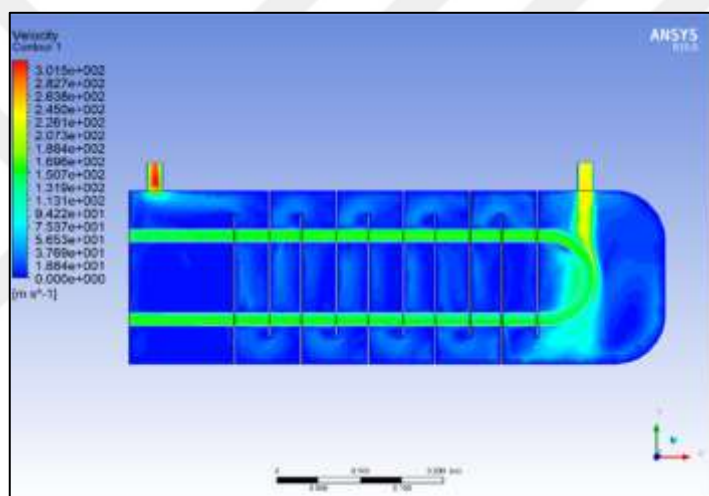


Figure 4.15: Velocity at 5 Pipes.

The results above found that the five-tube heat exchanger offers maximum heat exchange area and provides better heat transfer rate and performance with different friction factors. And the increasing number of pipes leads to an increase in all parameters, where the quantity of entering fluid passing through the system will be higher in 5 pipes. Because of the increasing number of pipes, the contact area between the working fluid and gas will increase, causing an increase in the heat transfer rate, velocity, pressure, and temperature of the system.

4.4 EFFECT OF TEMPERATURE

Temperature change is a significant consequence of heat transmission, wherein the process of heating results in an increase in temperature, while cooling induces a decrease in

temperature. The working temperature of the fluids as they traverse the exchanger exhibits variability along its entire span, with infrequent instances of constancy. The variability in the rate of heat transfer over the length of the exchanger tubes is attributed to the dependence of its value on the temperature variation among the hot and cold fluids at the specific site under observation. From the Figures 4.3 explain the effect of temperature change in heat exchanger, where three temperature degrees taken 745, 916 and 1055 oC, as shown.

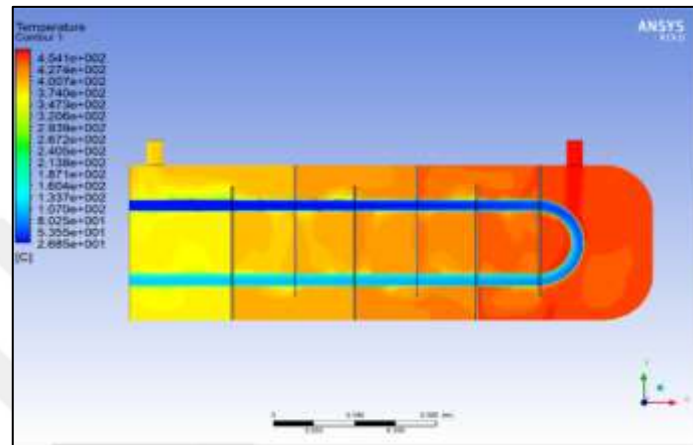


Figure 4.16: Temperature at 745 °C.

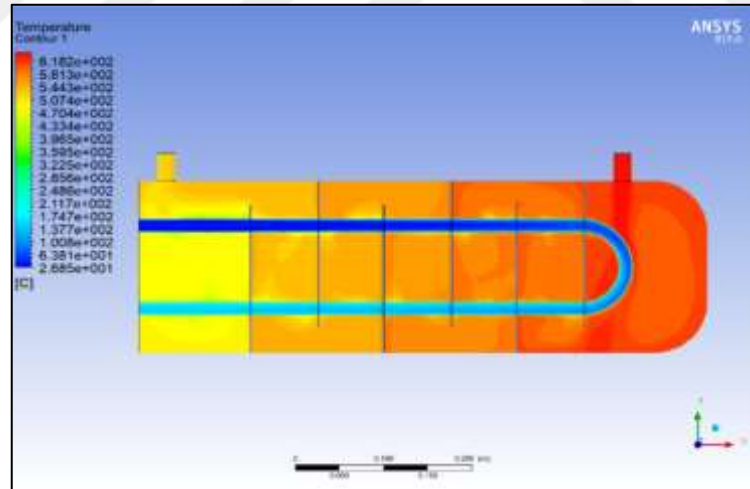


Figure 4.17: Temperature at 916 °C.

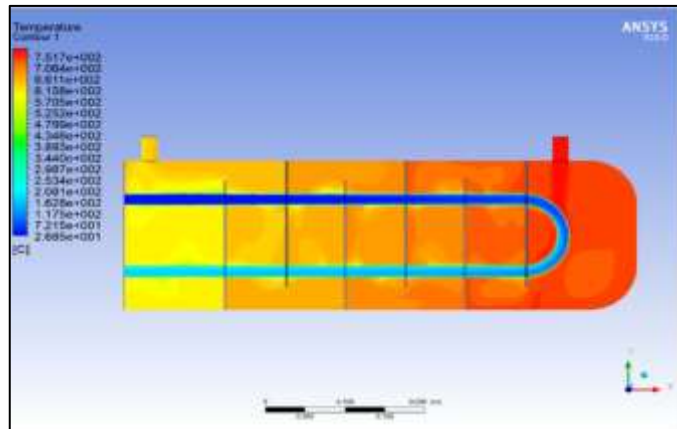


Figure 4.18: Temperature at 1055 °C.

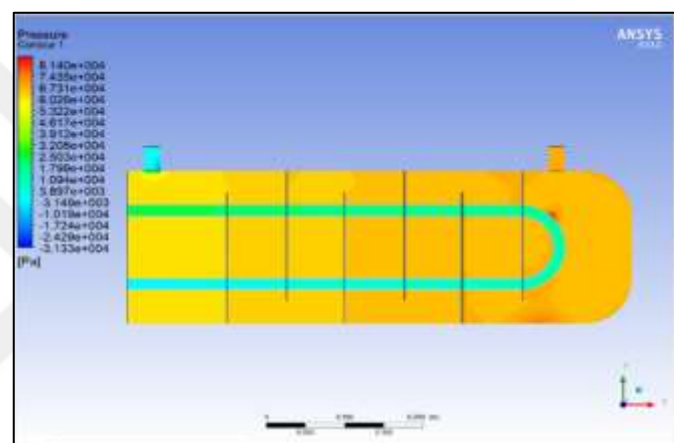


Figure 4.19: Pressure at 745 °C.

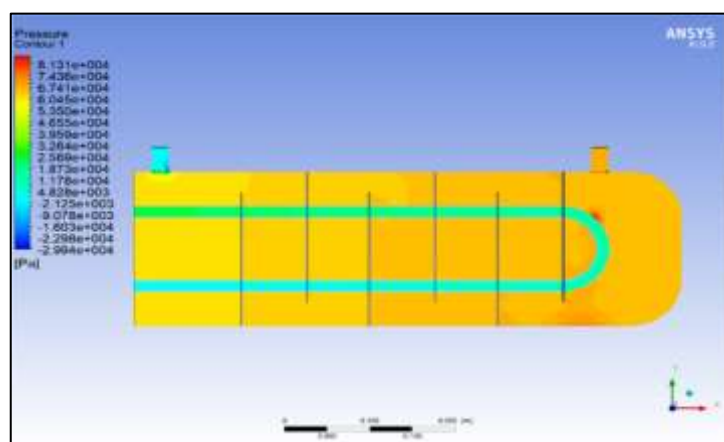


Figure 4.20: Pressure at 916 °C.

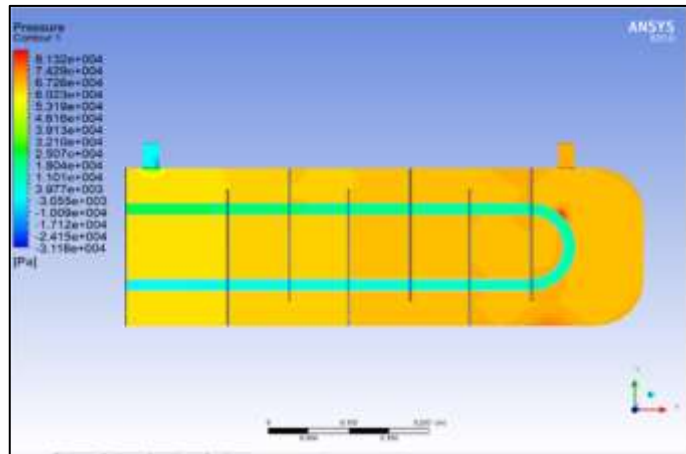


Figure 4.21: Pressure at 1055 °C.

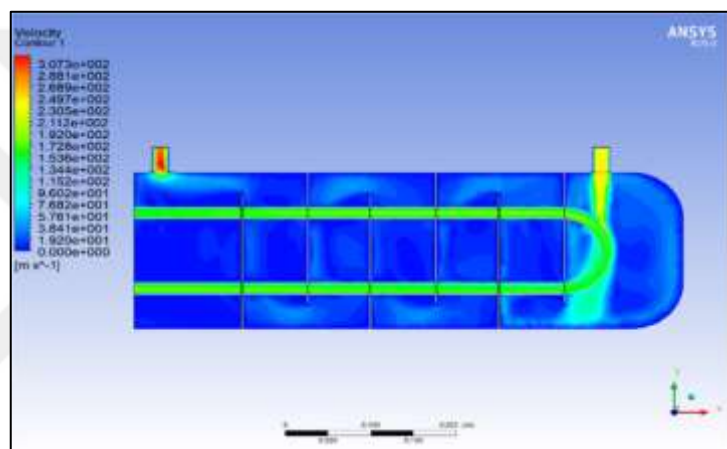


Figure 4.22: Velocity at 745 °C.

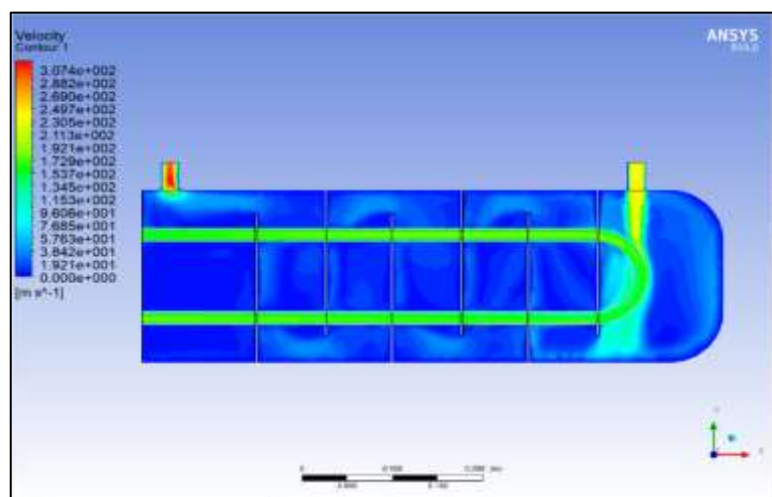


Figure 4.23: Velocity at 916 °C.

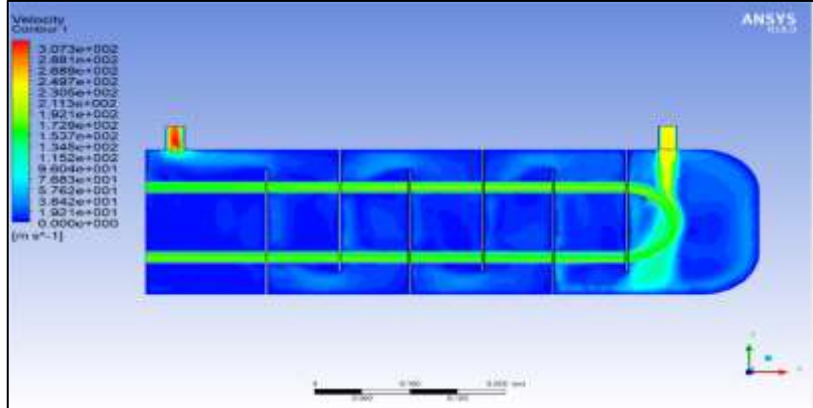


Figure 4.24: Velocity at 1055 °C.

The friction factor rose somewhat at low temperatures and more steeply at lower Reynolds numbers because of a rise in the Prandtl number and a drop in thermal conductivity, and it was discovered that the efficiency of heat transfer decreased progressively as temperature decreased. It also noticed that the increasing in temperature degrees influence clearly on the properties, where the temperature contour indicated good agreement with the increasing as shown at 1055 °C, which gives higher results than other degrees. While the velocity and pressure are little affected by the increase.

4.5 EFFECT OF PRESSURE

Phase changes and limited flow are the causes of pressure excursions. If a pump is transferring a process fluid into a heat exchanger, the pressure will rise upstream of the obstruction due to the reduced flow. The documentation of pressure decline through the heat exchanger is of significance in typical scenarios since an increase in pressure may result in flow restriction. If a pump is being utilized to move the process fluid through the heat exchanger, low pressure might also be a concern. In addition to employing a pressure gauge, the pump may have its vibration or current draw monitored. Additionally, the low flow may cause cavitation on the pump's input side. This may be checked out vocally or by measuring vibration signals using accelerometers.

In this study, two pressure values of 100 and 120 are selected to calculate the performance of the heat exchanger. These values are tested for different temperatures, baffles, and multi-pipes in the heat exchanger system, as shown in Figures 4.4.

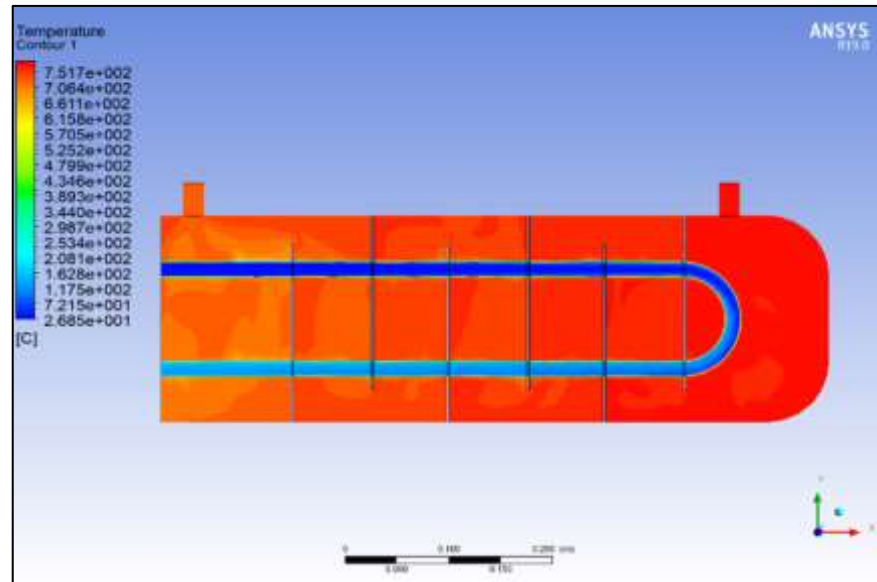


Figure 4.25: Temperature at 1055 °C + 100 ps.

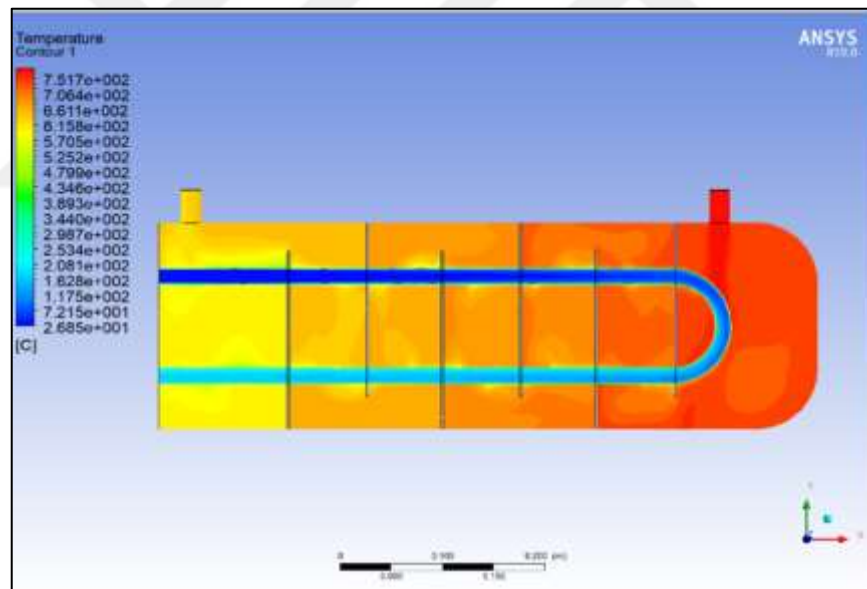


Figure 4.26: Temperature at 1055 °C + 120 ps.

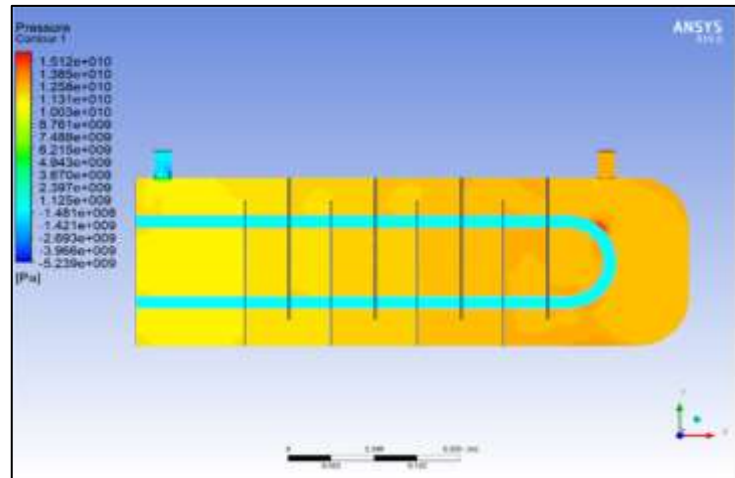


Figure 4.27: Pressure at 916 °C + 100 ps.

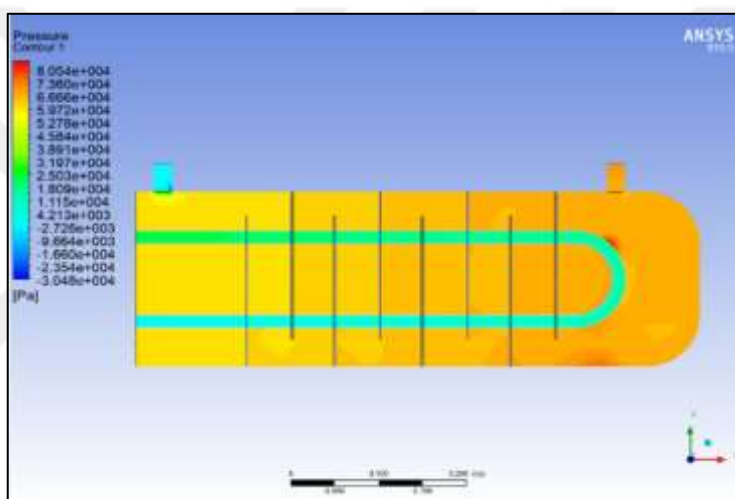


Figure 4.28: Pressure at 916 °C + 120 ps.

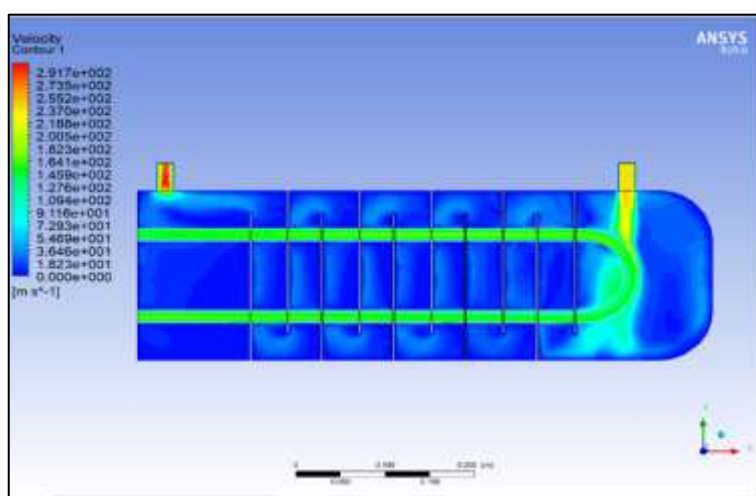


Figure 4.29: Velocity at 1055 °C + 100 ps.

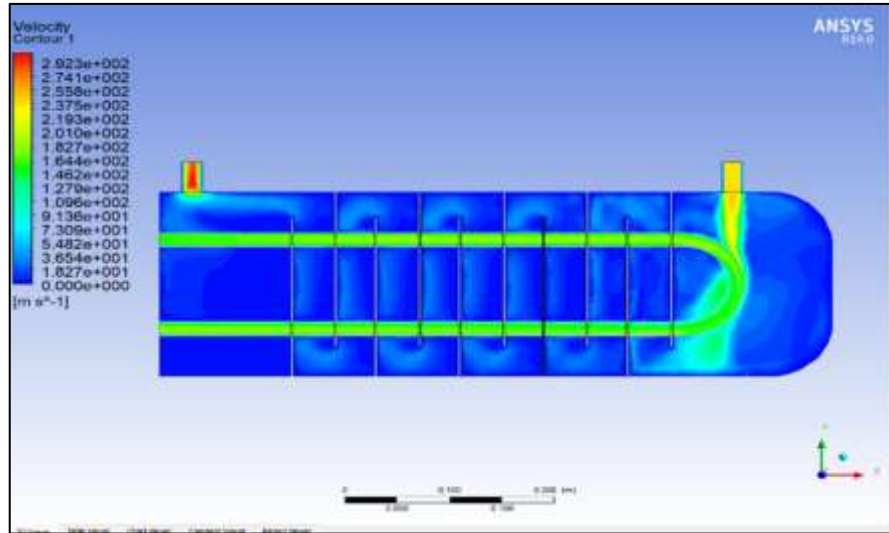


Figure 4.30: Velocity at 1055 °C + 120 ps.

Effects of operating pressure on heat exchangers: The pressure difference between each fluid stream's suction and discharge points is what propels it most. The pressure differential is influenced by several factors, including the number of passes through the heat exchanger, the variety of flows of fluid rates, bulk density, the friction pipe surface, and viscosity. The presence of deposits results in a reduction of the accessible surface area and an increase in the pressure differential, hence causing inadequate flow. The increase in fluid pressure inside the pipes causes an increase in heat. From Figure 4.4, there is little difference between the two pressures, whereas in a heat exchanger system, the main influencer parameter is temperature; therefore, the increase in pressure is smaller when compared with temperature.

4.6 OUTLET TEMPERATURE

The experiments done by ESS software can indicate the effect of increasing baffles on the outlet temperature of the heat exchanger for 100 and 120 Kpa pressure as its clear in Figure 4.5, where the temperature of the working fluid inside the system increased as the baffles increased.

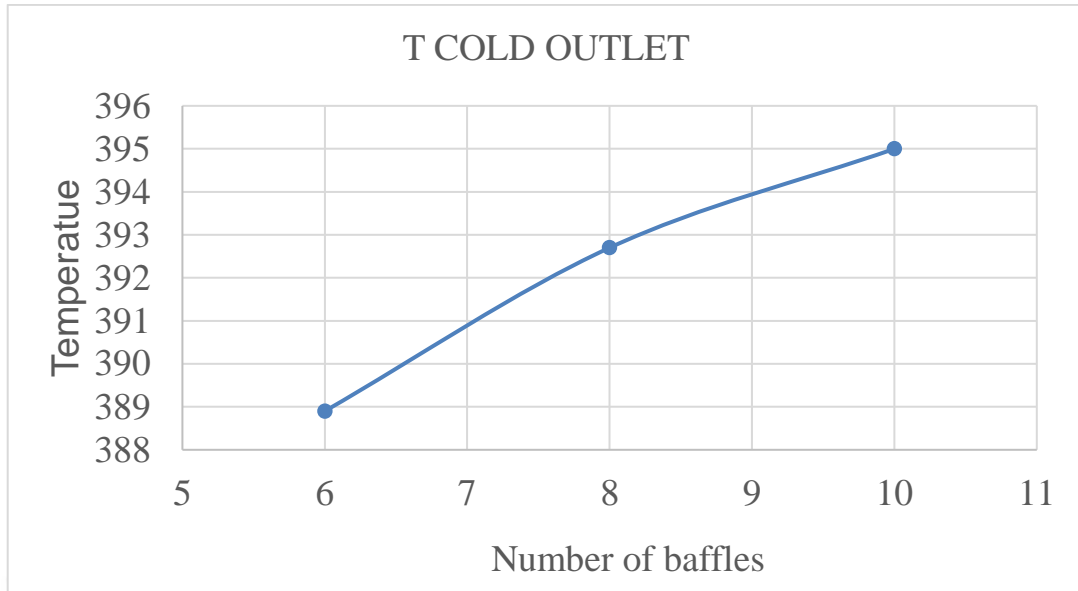


Figure 4.31: Outlet Temperature Diagram.

The increase reaches over 400 °C because the working fluid flows in a winding path through the pipes and takes a long time inside the system, causing an increase in heat transfer between the gas and fluid.

4.7 OVERALL EXERGY

Exergetic efficiency is the most crucial aspect to consider when assessing the thermal performance of an energy system. This parameter is given for an energy system as well as each of its parts. To assess and compare the energy efficiency, however, similar systems—not separate systems—must be looked at. For example, it is necessary to compare a turbine's energy efficiency to that of a similar turbine on the market to ascertain if the system is suitable from a thermal aspect. It suggests that it is inappropriate to compare the energy efficiency of different parts of an energy system, such as a power plant's turbine and boiler, in order to decide which, one is more effective. This is because, due to variations in technology and thermal processes, it is difficult to compare the energy efficiency of different systems. This rule applies to both the equipment (at the component level of an energy system) and the whole energy system. The strategy for optimizing an energy system using thermal criteria most often maximizes energetic efficiency as an objective function. The optimization of energy systems must be done using a holistic approach, however, since energetic optimization alone may undermine the economic case for employing the recommended energy system. In full optimization, thermal, economic, environmental,

reliability, and other factors must all be taken into consideration simultaneously. This study will determine the overall exergy of the exchanger system at a cold temperature to explain the performance of the system as shown in Figure 4.6.

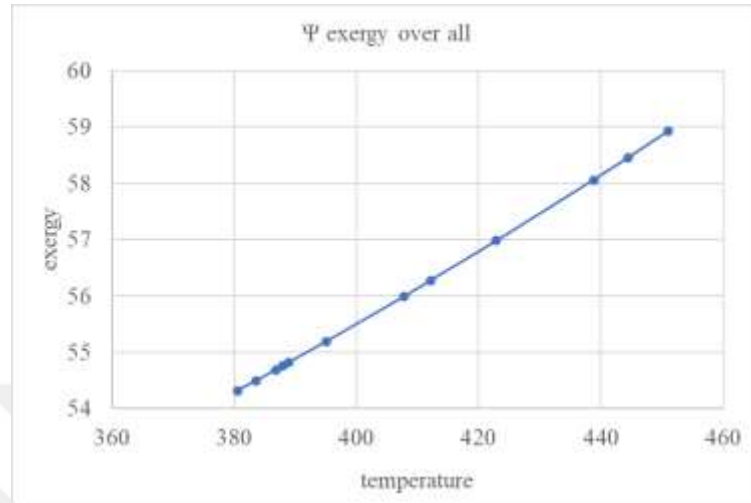


Figure 4.32: Exergy Diagram.

The overall exergy indicated moderately increasing behavior with temperature increasing, where the values were limited by 54 to 59 through all temperature degrees.

4.8 WORK

In this study, the work net was tested at cold temperatures to display the performance of the system as shown in Figure 4.7.

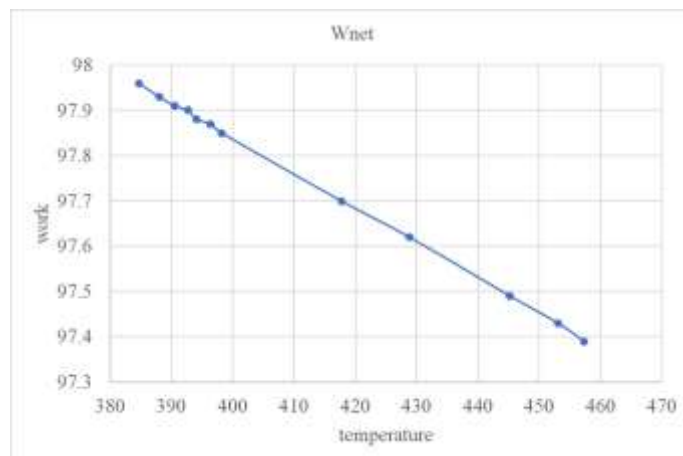


Figure 4.33: Work Net Diagram.

The work diagram indicated reverse behavior with temperature increasing, where at high temperatures the heat exchanger gives low work. Because the work produced by the system needs more heat energy, that has an effect on temperature.

4.9 ELECTRICITY

Utilizing solar energy, fossil fuels, or water to create electricity is the current trend in power plants. The energy transmission network is then used to deliver the power produced to the customers. Undoubtedly, a substantial investment is required for the transmission line due to the considerable distance between electrical power-producing facilities and consumers, which causes huge losses. The transmission network damage in these systems is another issue; as a result, electricity in one region will be lost until the problem is identified and fixed. In addition, severe emergency situations like a war or an earthquake often result in significant network damage. The electricity of the exchanger is affected by the temperature changes, as shown in Figure 4.8.

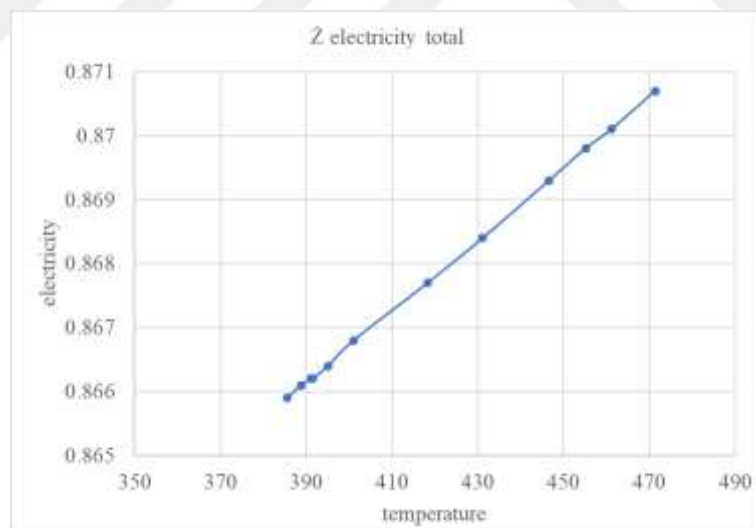


Figure 4.34: Electricity Diagram.

The higher the electricity obtained at a higher temperature degree because it depends on the temperature difference between the inlet and outlet of the system, when the difference is higher, the exchanger produces more electricity.

4.10 ENERGY OVERALL

A variety of approaches were looked at to enhance heat exchanger performance. The performance of a double-pipe heat exchanger entails enhancing the rate of heat transfer and preventing or reducing a significant pressure drop. Typically, a fluid with a high viscosity value is best suited for the side of the passageway with the largest area (annular), since this suggests a smaller pressure drop. The design, fluid characteristics, and kinds of flow are the key determinants of heat exchanger performance. The need for a large pump may be reduced without increasing the initial cost by reducing the pressure drop. Additionally, it lowers power use, which has an impact on operational expenses. Reduced speeds assist prevent erosion, tube vibrations, noise, and pressure decrease see Figure 4.9.

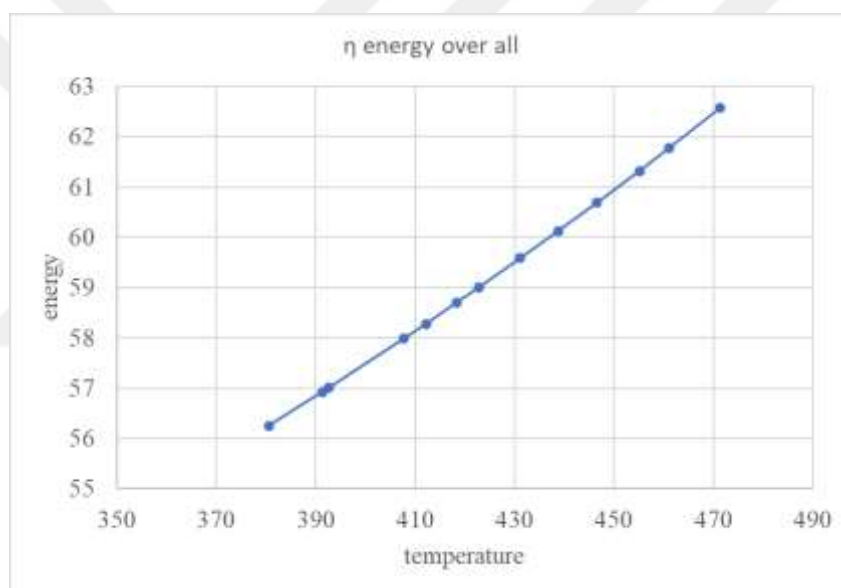


Figure 4.35: Overall Energy Diagram.

The performance of the thermal exchanger depends on many factors, like pressure, temperature, system design, and others. In this study, we will discuss the impact of the temperature factor. From the range of temperatures over 370 oC to 480 oC, we will notice that the thermal energy increases with temperature until it reaches over 62 because the highest temperature produces high heat energy, and that energy is proportional to overall performance.

5. CONCLUSION AND FUTURE WORKS

5.1 INTRODUCTION

This chapter explained the results that were concluded from the cases, where two types of heat exchangers (3 and 5 pipes) were taken to show the effect of increasing the pipe number in the system. The two exchangers were also tested at different temperatures (745, 916, and 1055 $^{\circ}\text{C}$) with three baffle numbers (6, 8, and 10) and under two pressures (100 and 120 kpa) to evaluate the velocity, pressure, and temperature of the working fluid. The system was designed by the ANSYS program, and the results that were extracted will be transferred to the EES program to study the performance, energy, electricity, and total work of the system at different temperatures.

From the results of the tests, it is concluded that. The results of the tested heat exchangers concluded that:

- i. Increasing the baffles in the system leads to an increase in heat transfer rate.
- ii. Heat exchangers with five pipes have higher performance than those with three pipes because the amount of inlet fluid will increase inside the system.
- iii. The highest temperature increases the thermal energy of the system because it increases the heat transfer between the working fluid and gas.
- iv. The effect of pressure on the results was denoted, where the highest pressure decreases the heat transfer rate because the fluid flow will be at high velocity inside the tubes.
- v. The overall energy of the system is 62.57 kW obtained highest temperature of 471.3 $^{\circ}\text{C}$, while the energy of the system is 60.42 kW at the same temperature.
- vi. The work net of the system ranged approximately between 97.28 and 97.99 kJ. also, the electricity because it's not affected deeply by the temperature change.
- vii. All properties of a system increase with temperature, except work, which is inversely proportional to heat.

5.2 RECOMMENDATIONS

The recommendations of this study are listed below:

- a. Inserting fins, coils, or twisted tape inside the pipes to increase the heat transfer rate.

- b. Adding nanoparticles to the working fluid to study the effects of hybrid nanofluids
- c. Studying the interaction between the fluid and the structure of the heat exchanger for different materials.



REFERENCES

- [1] L. Miró, J. Gasia, and L. F. Cabeza, “Thermal energy storage (TES) for industrial waste heat (IWH) recovery: A review,” *Appl. Energy*, vol. 179, pp. 284–301, 2016.
- [2] C. Forman, I. K. Muritala, R. Pardemann, and B. Meyer, “Estimating the global waste heat potential,” *Renew. Sustain. Energy Rev.*, vol. 57, pp. 1568–1579, 2016.
- [3] J. Guan, X. Lv, C. Spataru, and Y. Weng, “Experimental and numerical study on self-sustaining performance of a 30-kW micro gas turbine generator system during startup process,” *Energy*, vol. 236, p. 121468, 2021.
- [4] N. DeLovato, K. Sundarnath, L. Cvijovic, K. Kota, and S. Kuravi, “A review of heat recovery applications for solar and geothermal power plants,” *Renew. Sustain. Energy Rev.*, vol. 114, p. 109329, 2019.
- [5] A. Kumari, “Investigation of parameters affecting exergy and emission performance of basic and intercooled gas turbine cycles,” *Energy*, vol. 90, pp. 525–536, 2015.
- [6] L. Miró, S. Brückner, and L. F. Cabeza, “Mapping and discussing Industrial Waste Heat (IWH) potentials for different countries,” *Renew. Sustain. Energy Rev.*, vol. 51, pp. 847–855, 2015.
- [7] K. A. Abrosimov, A. Baccioli, and A. Bischi, “Techno-economic analysis of combined inverted Brayton–Organic Rankine cycle for high-temperature waste heat recovery,” *Energy Convers. Manag.*, vol. 207, p. 112336, 2020.
- [8] V. M. Maslennikov and V. J. Shterenberg, “Advanced gas turbine system utilizing partial oxidation technology for ecologically clean power generation,” *Int. J. Low-Carbon Technol.*, vol. 6, no. 1, pp. 55–63, 2011.
- [9] S. Taamallah, K. Vogiatzaki, F. M. Alzahrani, E. M. A. Mokheimer, M. A. Habib, and A. F. Ghoniem, “Fuel flexibility, stability and emissions in premixed hydrogen-rich gas turbine combustion: Technology, fundamentals, and numerical simulations,” *Appl. Energy*, vol. 154, pp. 1020–1047, 2015.
- [10] M. Alhuyi Nazari, M. Fahim Alavi, M. Salem, and M. E. H. Assad, “Utilization of

hydrogen in gas turbines: a comprehensive review," *Int. J. Low-Carbon Technol.*, vol. 17, no. April, pp. 513–519, 2022, doi: 10.1093/ijlct/ctac025.

[11] M. Ditaranto, H. Li, and Y. Hu, "Evaluation of a pre-combustion capture cycle based on hydrogen fired gas turbine with exhaust gas recirculation (EGR)," *Energy Procedia*, vol. 63, pp. 1972–1975, 2014.

[12] M. Faqih, M. B. Omar, R. Ibrahim, and B. A. A. Omar, "Dry-Low Emission Gas Turbine Technology: Recent Trends and Challenges," *Appl. Sci.*, vol. 12, no. 21, p. 10922, 2022.

[13] E. Agelidou, H. Seliger-Ost, M. Henke, V. Dreißigacker, T. Krummrein, and P. Kutne, "The Heat-Storing Micro Gas Turbine—Process Analysis and Experimental Investigation of Effects on Combustion," *Energies*, vol. 15, no. 17, p. 6289, 2022.

[14] X. Zhang, Y. Wu, W. Zhang, Q. Wang, and A. Wang, "System Performance and Pollutant Emissions of Micro Gas Turbine Combined Cycle in Variable Fuel Type Cases," *Energies*, vol. 15, no. 23, p. 9113, 2022.

[15] J. Najib, M. Nemer, and C. Bouallou, "Study of a Gas Turbine Cycle to Boost the Autonomy of Electric Cars," *Energies*, vol. 15, no. 9, p. 3348, 2022.

[16] R. De Robbio, "Micro gas turbine role in distributed generation with renewable energy sources," *Energies*, vol. 16, no. 2, p. 704, 2023.

[17] L. Herraiz, E. S. Fernández, E. Palfi, and M. Lucquiaud, "Selective exhaust gas recirculation in combined cycle gas turbine power plants with post-combustion CO₂ capture," *Int. J. Greenh. Gas Control*, vol. 71, pp. 303–321, 2018.

[18] M. Tahmasebzadehbaie, H. Sayyaadi, A. Sohani, and M. Z. Pedram, "Heat and mass recirculations strategies for improving the thermal efficiency and environmental emission of a gas-turbine cycle," *Appl. Therm. Eng.*, vol. 125, pp. 118–133, 2017.

[19] M. Anheden, "Analysis of gas turbine systems for sustainable energy conversion." Kemiteknik, 2000.

[20] Y. Du *et al.*, "Multi-objective optimization of an innovative power-cooling integrated

system based on gas turbine cycle with compressor inlet air precooling, Kalina cycle and ejector refrigeration cycle,” *Energy Convers. Manag.*, vol. 244, p. 114473, 2021.

[21] P. Ding, X. Liu, H. Qi, H. Shen, X. Liu, and S. G. Farkoush, “Multi-objective optimization of a new cogeneration system driven by gas turbine cycle for power and freshwater production,” *J. Clean. Prod.*, vol. 288, p. 125639, 2021.

[22] C. Uysal and A. Keçebaş, “Advanced exergoeconomic analysis with using modified productive structure analysis: an application for a real gas turbine cycle,” *Energy*, vol. 223, p. 120085, 2021.

[23] M. Zoghi, H. Habibi, A. Y. Choubari, and M. A. Ehyaei, “Exergoeconomic and environmental analyses of a novel multi-generation system including five subsystems for efficient waste heat recovery of a regenerative gas turbine cycle with hybridization of solar power tower and biomass gasifier,” *Energy Convers. Manag.*, vol. 228, p. 113702, 2021.

[24] M. G. Božo, S. Mashruk, S. Zitouni, and A. Valera-Medina, “Humidified ammonia/hydrogen RQL combustion in a trigeneration gas turbine cycle,” *Energy Convers. Manag.*, vol. 227, p. 113625, 2021.

[25] A. Görgülü, H. Yağlı, Y. Koç, and A. Koç, “Analysing the performance, fuel cost and emission parameters of the 50 MW,” *Int. J. Hydrogen Energy*, vol. 45, no. 58, pp. 34254–34267, 2020.

[26] Y. Koç, H. Yağlı, A. Görgülü, and A. Koc, “Analysing the performance, fuel cost and emission parameters of the 50 MW simple and recuperative gas turbine cycles using natural gas and hydrogen as fuel,” *Int. J. Hydrogen Energy*, vol. 45, no. 41, pp. 22138–22147, 2020.

[27] K. Mohammadi, K. Ellingwood, and K. Powell, “A novel triple power cycle featuring a gas turbine cycle with supercritical carbon dioxide and organic Rankine cycles: Thermo-economic analysis and optimization,” *Energy Convers. Manag.*, vol. 220, p. 113123, 2020.

[28] M. A. Budiyanto and R. Nawara, “The optimization of exergoenvironmental factors

in the combined gas turbine cycle and carbon dioxide cascade to generate power in LNG tanker ship," *Energy Convers. Manag.*, vol. 205, p. 112468, 2020.

[29] B. Zhang, Y. Chen, Z. Wang, and H. Shakibi, "Thermodynamic, environmental, and optimization of a new power generation system driven by a gas turbine cycle," *Energy Reports*, vol. 6, pp. 2531–2548, 2020.

[30] S. Mishra, A. Sharma, and A. Kumari, "Response surface methodology based optimization of air-film blade cooled gas turbine cycle for thermal performance prediction," *Appl. Therm. Eng.*, vol. 164, p. 114425, 2020.

[31] D. Mikielewicz *et al.*, "Gas turbine cycle with external combustion chamber for prosumer and distributed energy systems," *Energies*, vol. 12, no. 18, p. 3501, 2019.

[32] M. N. Khan and I. Tlili, "New approach for enhancing the performance of gas turbine cycle: A comparative study," *Results Eng.*, vol. 2, p. 100008, 2019.

[33] E. M. Leal, L. A. Bortolaia, and A. M. L. Junior, "Technical analysis of a hybrid solid oxide fuel cell/gas turbine cycle," *Energy Convers. Manag.*, vol. 202, p. 112195, 2019.

[34] R. Bontempo and M. Manna, "Work and efficiency optimization of advanced gas turbine cycles," *Energy Convers. Manag.*, vol. 195, pp. 1255–1279, 2019.

[35] G. Zhu, T. T. Chow, K. F. Fong, and C. K. Lee, "Comparative study on humidified gas turbine cycles with different air saturator designs," *Appl. Energy*, vol. 254, p. 113592, 2019.

[36] S. Jehandiseh, H. Hassanzadeh, and S. E. Shakib, "Environmental assessment of a hybrid system composed of solid oxide fuel cell, gas turbine and multiple effect evaporation desalination system," *Energy Environ.*, vol. 32, no. 5, pp. 874–901, 2021.

[37] M. Zoghi, H. Habibi, A. Chitsaz, and M. Shamsaiee, "Exergoeconomic and environmental analyses of a novel trigeneration system based on combined gas turbine-air bottoming cycle with hybridization of solar power tower and natural gas combustion," *Appl. Therm. Eng.*, vol. 188, p. 116610, 2021.

[38] Y. Cao, H. A. Dhahad, H. Togun, A. E. Anqi, N. Farouk, and B. Farhang, “A novel hybrid biomass-solar driven triple combined power cycle integrated with hydrogen production: Multi-objective optimization based on power cost and CO₂ emission,” *Energy Convers. Manag.*, vol. 234, p. 113910, 2021.

[39] S. Cen, K. Li, Q. Liu, and Y. Jiang, “Solar energy-based hydrogen production and post-firing in a biomass fueled gas turbine for power generation enhancement and carbon dioxide emission reduction,” *Energy Convers. Manag.*, vol. 233, p. 113941, 2021.

[40] S. E. Shakib, M. Amidpour, M. Boghrati, M. M. Ghafurian, and A. Esmaieli, “New approaches to low production cost and low emissions through hybrid MED-TVC+ RO desalination system coupled to a gas turbine cycle,” *J. Clean. Prod.*, vol. 295, p. 126402, 2021.

[41] S. Wang *et al.*, “Techno-economic-environmental evaluation of a combined cooling heating and power system for gas turbine waste heat recovery,” *Energy*, vol. 231, p. 120956, 2021.

[42] M. R. M. Yazdi, F. Ommi, M. A. Ehyaei, and M. A. Rosen, “Comparison of gas turbine inlet air cooling systems for several climates in Iran using energy, exergy, economic, and environmental (4E) analyses,” *Energy Convers. Manag.*, vol. 216, p. 112944, 2020.

[43] M. A. Javadi, S. Hoseinzadeh, R. Ghasemiasl, P. S. Heyns, and A. J. Chamkha, “Sensitivity analysis of combined cycle parameters on exergy, economic, and environmental of a power plant,” *J. Therm. Anal. Calorim.*, vol. 139, pp. 519–525, 2020.

[44] A. Khaliq, M. A. Habib, and K. Choudhary, “A thermo-environmental evaluation of a modified combustion gas turbine plant,” *J. Energy Resour. Technol.*, vol. 141, no. 4, p. 42004, 2019.

[45] Y. Liu, X. Sun, V. Sethi, D. Nalianda, Y.-G. Li, and L. Wang, “Review of modern low emissions combustion technologies for aero gas turbine engines,” *Prog. Aerosp. Sci.*, vol. 94, pp. 12–45, 2017.

[46] M. Ditaranto, H. Li, and T. Løvås, “Concept of hydrogen fired gas turbine cycle with exhaust gas recirculation: Assessment of combustion and emissions performance,” *Int. J. Greenh. Gas Control*, vol. 37, pp. 377–383, 2015.

[47] B. Najafi, A. Shirazi, M. Aminyavari, F. Rinaldi, and R. A. Taylor, “Exergetic, economic and environmental analyses and multi-objective optimization of an SOFC-gas turbine hybrid cycle coupled with an MSF desalination system,” *Desalination*, vol. 334, no. 1, pp. 46–59, 2014.

[48] A. G. Memon, K. Harijan, M. A. Uqaili, and R. A. Memon, “Thermo-environmental and economic analysis of simple and regenerative gas turbine cycles with regression modeling and optimization,” *Energy Convers. Manag.*, vol. 76, pp. 852–864, 2013.

[49] A. M. Elkady *et al.*, “Gas turbine emission characteristics in perfectly premixed combustion,” 2012.

[50] S. Sattar *et al.*, “Corrosion reduction in steam turbine blades using nano-composite coating,” *J. King Saud Univ.*, vol. 35, no. 8, p. 102861, 2023.

[51] P. Ahmadi, M. A. Rosen, and I. Dincer, “Greenhouse gas emission and exergo-environmental analyses of a trigeneration energy system,” *Int. J. Greenh. Gas Control*, vol. 5, no. 6, pp. 1540–1549, 2011.

[52] S. Soltani, S. M. S. Mahmoudi, M. Yari, and M. A. Rosen, “Thermodynamic analyses of an externally fired gas turbine combined cycle integrated with a biomass gasification plant,” *Energy Convers. Manag.*, vol. 70, pp. 107–115, 2013.

[53] F. Zabihian and A. S. Fung, “Performance analysis of hybrid solid oxide fuel cell and gas turbine cycle: application of alternative fuels,” *Energy Convers. Manag.*, vol. 76, pp. 571–580, 2013.

[54] M. J. Santos, R. P. Merchán, A. Medina, and A. C. Hernández, “Seasonal thermodynamic prediction of the performance of a hybrid solar gas-turbine power plant,” *Energy Convers. Manag.*, vol. 115, pp. 89–102, 2016.

[55] S. Hou, Y. Wu, Y. Zhou, and L. Yu, “Performance analysis of the combined supercritical CO₂ recompression and regenerative cycle used in waste heat recovery

of marine gas turbine,” *Energy Convers. Manag.*, vol. 151, pp. 73–85, 2017.

[56] S. Wang, C. Liu, J. Li, Z. Sun, X. Chen, and X. Wang, “Exergoeconomic analysis of a novel trigeneration system containing supercritical CO₂ Brayton cycle, organic Rankine cycle and absorption refrigeration cycle for gas turbine waste heat recovery,” *Energy Convers. Manag.*, vol. 221, p. 113064, 2020.

[57] H. Sayyaadi and R. Mehrabipour, “Efficiency enhancement of a gas turbine cycle using an optimized tubular recuperative heat exchanger,” *Energy*, vol. 38, no. 1, pp. 362–375, 2012.

[58] A. Shirazi, B. Najafi, M. Aminyavari, F. Rinaldi, and R. A. Taylor, “Thermal–economic–environmental analysis and multi-objective optimization of an ice thermal energy storage system for gas turbine cycle inlet air cooling,” *Energy*, vol. 69, pp. 212–226, 2014.

[59] S. Dybe, F. Gütthe, M. Bartlett, P. Stathopoulos, and C. O. Paschereit, “Experimental Characterization of the Combustion in Fuel Flexible Humid Power Cycles,” in *Turbo Expo: Power for Land, Sea, and Air*, 2021, vol. 84942, p. V03AT04A012.

[60] S. K. Cho, M. Kim, S. Baik, Y. Ahn, and J. I. Lee, “Investigation of the bottoming cycle for high efficiency combined cycle gas turbine system with supercritical carbon dioxide power cycle,” in *turbo expo: Power for land, sea, and air*, 2015, vol. 56802, p. V009T36A011.

[61] M. Mohammadpour, E. Houshfar, M. Ashjaee, and A. Mohammadpour, “Energy and exergy analysis of biogas fired regenerative gas turbine cycle with CO₂ recirculation for oxy-fuel combustion power generation,” *Energy*, vol. 220, p. 119687, 2021.

[62] M. Ditaranto, T. Heggset, and D. Berstad, “Concept of hydrogen fired gas turbine cycle with exhaust gas recirculation: Assessment of process performance,” *Energy*, vol. 192, p. 116646, 2020.

[63] J.-M. Bellas, K. N. Finney, M. E. Diego, D. Ingham, and M. Pourkashanian, “Experimental investigation of the impacts of selective exhaust gas recirculation on a micro gas turbine,” *Int. J. Greenh. Gas Control*, vol. 90, p. 102809, 2019.

[64] S. Hasemann, A. Huber, C. Naumann, and M. Aigner, “Investigation of a FLOX®-based combustor for a micro gas turbine with exhaust gas recirculation,” in *Turbo Expo: Power for Land, Sea, and Air*, 2017, vol. 50855, p. V04BT04A012.

[65] M. Tahmasebzadehbaie and H. Sayyaadi, “Efficiency enhancement and NO_x emission reduction of a turbo-compressor gas engine by mass and heat recirculations of flue gases,” *Appl. Therm. Eng.*, vol. 99, pp. 661–671, 2016.

[66] A. A. Taimoor, A. Muhammad, and W. Saleem, “Humidified exhaust recirculation for efficient combined cycle gas turbines,” *Energy*, vol. 106, pp. 356–366, 2016.

[67] A. De Santis, D. B. Ingham, L. Ma, and M. Pourkashanian, “CFD analysis of exhaust gas recirculation in a micro gas turbine combustor for CO₂ capture,” *Fuel*, vol. 173, pp. 146–154, 2016.

[68] U. Ali, C. F. Palma, K. J. Hughes, D. B. Ingham, L. Ma, and M. Pourkashanian, “Impact of the operating conditions and position of exhaust gas recirculation on the performance of a micro gas turbine,” in *Computer Aided Chemical Engineering*, vol. 37, Elsevier, 2015, pp. 2417–2422.

[69] U. Ali *et al.*, “Process simulation and thermodynamic analysis of a micro turbine with post-combustion CO₂ capture and exhaust gas recirculation,” *Energy Procedia*, vol. 63, pp. 986–996, 2014.

[70] R. Canepa, M. Wang, C. Biliyok, and A. Satta, “Thermodynamic analysis of combined cycle gas turbine power plant with post-combustion CO₂ capture and exhaust gas recirculation,” *Proc. Inst. Mech. Eng. Part E J. Process Mech. Eng.*, vol. 227, no. 2, pp. 89–105, 2013.

[71] B. Belaissaoui, G. Cabot, M.-S. Cabot, D. Willson, and E. Favre, “An energetic analysis of CO₂ capture on a gas turbine combining flue gas recirculation and membrane separation,” *Energy*, vol. 38, no. 1, pp. 167–175, 2012.

[72] F. Sander, R. Carroni, S. Rofka, and E. Benz, “Flue gas recirculation in a gas turbine: Impact on performance and operational behavior,” in *Turbo Expo: Power for Land, Sea, and Air*, 2011, vol. 54648, pp. 123–132.

[73] H. Li, G. Haugen, M. Ditaranto, D. Berstad, and K. Jordal, “Impacts of exhaust gas recirculation (EGR) on the natural gas combined cycle integrated with chemical absorption CO₂ capture technology,” *Energy Procedia*, vol. 4, pp. 1411–1418, 2011.

[74] A. M. Steinberg, I. Boxx, M. Stöhr, C. D. Carter, and W. Meier, “Flow–flame interactions causing acoustically coupled heat release fluctuations in a thermoacoustically unstable gas turbine model combustor,” *Combust. Flame*, vol. 157, no. 12, pp. 2250–2266, 2010.

